Published in final edited form as:
Deep Sea Res Part 2 Top Stud Oceanogr. 2014 May 1; 103: 139–162. doi:10.1016/j.dsr2.2013.06.022.

Diversity and toxicity of the diatom *Pseudo-nitzschia* Peragallo in the Gulf of Maine, Northwestern Atlantic Ocean

Luciano F. Fernandes[a,*], **Katherine A. Hubbard**[b,c,*], **Mindy L. Richlen**[b], **Juliette Smith**[b], **Stephen S. Bates**[d], **James Ehrman**[e], **Claude Léger**[d], **Luiz L. Mafra Jr.**[f], **David Kulis**[b], **Michael Quilliam**[g], **Katie Libera**[b], **Linda McCauley**[b], and **Donald M. Anderson**[b]

[a]Universidade Federal do Paraná, Centro Politécnico, Department of Botany, Curitiba, Paraná, CEP 81531-990, Brazil

[b]Woods Hole Oceanographic Institution, Department of Biology, MS-32, Woods Hole, MA 02536, USA

[c]Fish and Wildlife Research Institute, Florida Fish and Wildlife Conservation Commission, 100 8th Ave SE, St. Petersburg, FL, 33701, USA

[d]Fisheries and Oceans Canada, Gulf Fisheries Centre, 343 av. Université, Moncton, NB, E1C 9B6, Canada

[e]Digital Microscopy Facility, Mount Allison University, Sackville, NB, E4L 1G7, Canada

[f]Universidade Federal do Paraná, Center for Marine Studies, Pontal do Paraná, PR, 83255-976, Brazil

[g]National Research Council of Canada, Biotoxin Metrology, Measurement Science and Standards, 1411 Oxford Street, Halifax, Nova Scotia B3H 3Z1, Canada

Abstract

Multiple species in the toxic marine diatom genus *Pseudo-nitzschia* have been identified in the Northwestern Atlantic region encompassing the Gulf of Maine (GOM), including the Bay of Fundy (BOF). To gain further knowledge of the taxonomic composition and toxicity of species in this region, *Pseudo-nitzschia* isolates (n=146) were isolated from samples collected during research cruises that provided broad spatial coverage across the GOM and the southern New England shelf, herein referred to as the GOM region, during 2007-2008. Isolates, and cells in field material collected at 38 stations, were identified using electron microscopy (EM). Eight species (*P. americana, P. fraudulenta, P. subpacifica, P. heimii, P. pungens, P. seriata, P. delicatissima* and *P. turgidula*), and a novel form, *Pseudo-nitzschia* sp. GOM, were identified. Species identity was confirmed by sequencing the large subunit of the ribosomal rDNA (28S) and the internal transcribed spacer 2 (ITS2) for six species (36 isolates). Phylogenetic analyses (including neighbor

Corresponding Author: Katherine.Hubbard@MyFWC.com (Katherine Hubbard).
*The first and second authors contributed equally to the project.

joining, maximum parsimony, and maximum likelihood estimates and ITS2 secondary structure analysis) and morphometric data supported the placement of *P*. sp. GOM in a novel clade that includes morphologically and genetically similar isolates from Australia and Spain and is genetically most similar to *P. pseudodelicatissima* and *P. cuspidata*. Seven species (46 isolates) were grown in nutrient-replete batch culture and aliquots consisting of cells and growth medium were screened by Biosense ASP ELISA to measure total domoic acid (DA) produced (intracellular + extracellular); *P. americana* and *P. heimii* were excluded from all toxin analyses as they did not persist in culture long enough for testing. All 46 isolates screened produced DA in culture and total DA varied among species (e.g., 0.04 to 320 ng ml^{-1} for *P. pungens* and *P*. sp. GOM isolates, respectively) and among isolates of the same species (e.g., 0.24 – 320 ng ml^{-1} for *P*. sp. GOM). The 15 most toxic isolates corresponded to *P. seriata, P*. sp. GOM and *P. pungens*, and fg DA $cell^{-1}$ was determined for whole cultures (cells and medium) using ELISA and liquid chromatography (LC) with fluorescence detection (FLD); for seven isolates, toxin levels were also estimated using LC - with mass spectrometry and ultraviolet absorbance detection. *Pseudo-nitzschia seriata* was the most toxic species (up to 3,500 fg $cell^{-1}$) and was observed in the GOM region during all cruises (i.e., during the months of April, May, June and October). *Pseudo-nitzschia* sp. GOM, observed only during September and October 2007, was less toxic (19 – 380 fg $cell^{-1}$) than *P. seriata* but more toxic than *P. pungens* var. *pungens* (0. 4 fg $cell^{-1}$). Quantitation of DA indicated that concentrations measured by LC and ELISA were positively and significantly correlated; the lower detection limit of the ELISA permitted quantification of toxicity in isolates that were found to be nontoxic with LC methods. The confirmation of at least seven toxic species and the broad spatial and temporal distribution of toxic *Pseudo-nitzschia* spp. have significant implications for the regional management of nearshore and offshore shellfisheries resources.

Keywords

Pseudo-nitzschia; Gulf of Maine; Bay of Fundy; Georges Bank; harmful algal blooms; species diversity; domoic acid; Amnesic Shellfish Poisoning

1. Introduction

The Gulf of Maine (GOM) encompasses an extensive area of the continental shelf of the northeastern United States and Canada, including Georges Bank and the Bay of Fundy (BOF). Currents in the GOM are complex and reflect distinct source waters, with the Maine Coastal current being the main physico-chemical driver in coastal waters (Pettigrew et al., 2005). Tidal processes contribute to vertical mixing of nutrients and the waters of the GOM support elevated phytoplankton growth rates, resulting in high biological productivity (Thomas et al., 2003; Townsend et al., 2010a). The high levels of primary production observed seasonally in coastal regions, and throughout the year in offshore well-mixed areas like Georges Bank, support extensive and commercially important shellfisheries and fisheries, and provide feeding grounds for a number of migratory apex predators including cetacean and pinniped species (Kenney and Winn, 1986; Waring et al., 2012).

Several harmful algal bloom (HAB) species occurring within the GOM system are known to produce neurotoxins that have the potential to threaten human and ecosystem health (Li et al., 2011). One of the most comprehensively studied HAB species in the GOM is the toxic

dinoflagellate *Alexandrium fundyense* Balech, which produces a suite of neurotoxins that can cause paralytic shellfish poisoning (PSP) when contaminated seafood is consumed by humans. The annual occurrence of *A. fundyense* blooms necessitates closures of shellfish harvests to protect human health, usually from early May to late July, which in some years span the entire New England coastline (Kleindinst et al., this issue). In addition to the public health threat, closures of shellfish beds can also result in considerable losses to local economies dependent on the shellfish industry and tourism (Bean et al., 2005; McGillicuddy et al., 2005).

A separate group of harmful algae present in the GOM includes multiple species of the diatom genus *Pseudo-nitzschia* H. Peragallo that can produce the neurotoxin domoic acid (DA). This toxin accumulates in filter-feeding bivalves or fish, and when consumed via these vectors, causes amnesic shellfish poisoning (ASP) in humans or domoic acid poisoning (DAP) in marine wildlife, including mammals, seabirds and some fish (see Lefebvre and Robertson, 2010; Lelong et al., 2012; Trainer et al., 2012). Symptoms of ASP in humans include vomiting, diarrhea, abdominal cramps and neurological complications such as headaches, loss of short-term memory, respiratory malfunctions, coma or death (FAO, 2004). The first and only known ASP event that resulted in human mortality occurred north of the GOM in eastern Canada in 1987. Over 107 people were sickened and several died from eating DA-contaminated shellfish collected from Prince Edward Island (PEI) during a bloom of *P. multiseries* (Perl et al., 1990). Since this event, blooms of potentially toxic *Pseudo-nitzschia* species have been increasingly reported and are now known to occur globally (see reviews of FAO, 2004; Lelong et al., 2012; Trainer et al., 2012), prompting local, federal and international agencies to adopt specific public health regulations and marine biotoxin monitoring programs with respect to DA and ASP.

In the United States (U.S.), Canada and the European Union, the regulatory limit for DA in bivalves for human consumption has been set at 20 ppm (20 μg DA g^{-1} shellfish tissue) in order to minimize the threat of acute DA exposure and ASP. International and national regulatory activities range from the routine enumeration and/or identification of phytoplankton in field samples to the quantification of toxins in animal tissue (e.g., shellfish, finfish) using a variety of methods, including advanced analytical instrumentation, biochemical assays, and now less frequently, animal bioassays. In eastern Canadian waters, shellfish samples are collected and screened for DA routinely by the Canadian Food Inspection Agency (CFIA), and phytoplankton monitoring has been conducted at certain locations by varied agencies (Bates, 2004; Martin et al., 1990), although this is now diminished. Since the 1987 ASP event on PEI, a series of ASP closures have occurred in eastern Canada in the waters of Quebec, New Brunswick, PEI, Nova Scotia and Newfoundland (Trainer et al., 2012). In the U.S., shellfish managers in each state partner with local and/or federal public health agencies and work within the National Shellfish Sanitation Program to conduct sampling and biotoxin analysis. States bordering the GOM currently conduct adaptive sampling for DA; collection of shellfish material for regulatory DA testing is triggered when local phytoplankton monitoring groups identify potentially hazardous levels of *Pseudo-nitzschia* spp. in water samples that also test positive for DA with the ASP Jellett Rapid Testing kit. Most offshore U.S. waters, including Georges Bank,

fall under federal jurisdiction and are managed by the U.S. Food and Drug Administration, primarily for PSP toxins at this time (DeGrasse et al., this issue). Other states, including those along the U.S. west coast where DA closures occur regularly (Lewitus et al., 2012; Trainer et al., 2009a; Trainer et al., 2009b), conduct routine shellfish flesh testing for DA. To our knowledge, levels in excess of 20 jig DA g^{-1} in edible shellfish tissue have not yet been detected in nearshore GOM waters (Gilgan et al., 1990), although shellfish collected from offshore waters exceeded regulatory limits in 1995 (Stewart et al., 1998) and toxigenic species have been identified throughout the GOM (Leandro et al., 2010; Villareal et al., 1994).

Pseudo-nitzschia spp. were first described in GOM phytoplankton assemblages in the 1920s and 1930s in the Georges Bank region (Gran, 1933; Gran and Braarud, 1935; Lillick, 1940) and in the vicinity of Cape Cod (Fish, 1925; Lillick, 1937). Decades later, *Pseudo-nitzschia* spp. were observed throughout the GOM and its adjacent waters (Marshall, 1984; Marshall and Cohn, 1981; Marshall and Cohn, 1981; 1982, 1983, 1987). Most of these early reports of *Pseudo-nitzschia* spp. describe the presence of three species in the region (*P. delicatissima, P. pungens* and *P. seriata*) based on observations conducted with light microscopy (LM). However, many *Pseudo-nitzschia* species share cryptic morphological characteristics that are not readily observed with LM. Instead, electron microscopy and/or molecular approaches are often necessary for species identification and have been used in tandem to discriminate several novel *Pseudo-nitzschia* species within the past 15 years (see Amato and Montresor, 2008; Lelong et al., 2012; Lim et al., 2012; Lundholm et al., 2002, 2003, 2012; Trainer et al., 2012; Villac and Fryxell, 1998). These approaches have been used to identify additional *Pseudo-nitzschia* species diversity in waters of the GOM, including the Bay of Fundy (BOF). Using EM, Villareal et al. (1994) and Hargraves and Maranda (2002) described three species (*P. pungens, P. multiseries* and *P. pseudodelicatissima*), with the latter study recording three additional species (*P. delicatissima, P. fraudulenta* and *P. seriata*). Additional species in the *P. pseudodelicatissima*-complex have been observed (based on morphological and genetic features), including *P. calliantha, P. cuspidata* and *P. hasleana* (Kaczmarska et al., 2005; Kaczmarska et al., 2007; Kaczmarska et al., 2008; Leandro et al., 2010; Lundholm et al., 2012); morphological variants *P.* cf. *turgidula* and *P.* cf. *calliantha* were also described in previous regional studies (Leandro et al., 2010; Lundholm et al., 2003). At least 13 of the 38 *Pseudo-nitzschia* species described globally are capable of producing DA (Lelong et al., 2012), although species composition and species toxicity vary from region to region (Trainer et al., 2012). Although toxin production has been observed in several of these species globally, few GOM/BOF isolates (Martin et al., 1990) have been tested directly and regional variability in toxicity is commonly reported in the literature (Trainer et al., 2012).

Here, we combined sensitive detection capabilities for species identification, using electron microscopy in tandem with DNA sequencing, and toxin quantitation, using enzyme-linked immunosorbent assay (ELISA), and liquid chromatography (LC) coupled with mass spectrometry (LC-MS), ultraviolet detection (LC-UVD) or fluorescence (LC-FLD) detection, to consider the diversity, toxicity, and spatial and temporal occurrence of *Pseudo-nitzschia* species in the GOM region. This work is an important first step towards achieving

a greater understanding of the population dynamics and toxicity of regional *Pseudo-nitzschia* spp. and of the potential implications for human and ecosystem health and management of shellfish resources.

2. Material and Methods

2.1 Sample collection

Samples for cell isolation were collected during several large-scale research cruises in the GOM and nearby areas, including the southern New England shelf, as well as in cooperation with a number of state and local agencies (see below); sampling locations are shown in Figure 1. Most samples were collected from coastal and offshore areas throughout this greater region, herein referred to as the GOM region, during research cruises from October 08 - 18, 2007, April 28 - May 5, 2008 and May 27 - June 04, 2008. Coastal samples were also obtained in coordination with the Volunteer Phytoplankton Monitoring Networks in Maine and New Hampshire, and the Massachusetts Department of Marine Fisheries, as well the Massachusetts Water Resource Authority. In addition to the broad spatial coverage provided by these varied cruises, sampling efforts spanned two years (2007-2008) and three seasons (spring, summer and fall). Latitude and longitude coordinates for all isolates are provided in Table S1.

2.1 Cell isolation and culturing

The cultures established and used in this project originated from cell isolations performed following each sampling effort. For the isolations, seawater was collected through the bow pump, or from a surface bucket grab. An aliquot of either whole or concentrated (with a 10-μm mesh sieve) seawater was added to a 50 ml tissue culture flask. An aliquot of f/2 plus silicate culture medium was added to each flask, achieving a final medium concentration of f/16. While onboard the ship, samples were incubated at approximately the ambient seawater temperature and under low light levels. Upon return to the laboratory, individual *Pseudo-nitzschia* cells or chains were isolated by micropipette and placed into 96-well plates containing 200 μl of f/2 medium. Throughout the isolation process, isolates were maintained in an incubator at 10 °C, under an irradiance of at least 100 μmol photons m^{-2} s^{-1}, with a 12:12 hour light:dark cycle. Newly isolated cells were incubated in plates for several weeks. Successful isolates were transferred into 50-ml culture flasks containing 25 ml of f/2 medium and were maintained under the above growth conditions. Cell growth was assessed by visual inspection with LM.

2.2 Morphological identification of species

Cells were harvested during the exponential growth phase and preserved in Lugol's solution (1%) until morphometrics were obtained. A total of 154 *Pseudo-nitzschia* isolates, plus field material from each cruise, was examined using an Olympus BX-50 microscope. A subset of isolates and field samples, selected to encompass the morphological diversity observed with LM (Table 1), was prepared for scanning electron microscopy (SEM) following Kaczmarska et al. (2005) and examined using a JEOL JSM-5600 SEM operating at 10 kV and 8 mm working distance. Transmission electron microscopy (TEM) was conducted on isolates that were not readily identified by LM/SEM. For TEM, one drop of a cleaned sample was placed

on Formvar/carbon-coated nickel grids, dried at 35 °C, and visualized with a JEOL 1200 EXII electron microscope. Frustule measurements, including number of interstriae, poroids and fibulae, and number of poroids in the girdle bands of the cingulum, were conducted at the middle of the valve.

2.3 DNA extraction, amplification and sequencing

In addition to the morphological analyses, cultures examined using EM were also identified genetically by sequencing portions of their ribosomal RNA genes (rRNA), specifically the D1-D3 hypervariable region of the large subunit (LSU) rRNA (Scholin et al., 1994) and the internal transcribed spacer (ITS2) region. DNA was extracted from 200 µl of dense culture at exponential growth phase using the Generation Capture Column Kit (Qiagen, Valencia, CA, USA), following the manufacturer's instructions, with a final elution volume of 200 µl. The LSU rRNA was amplified using primers D1R and D3Ca (Scholin et al., 1994), and the ITS2 region was amplified using primers ITS-03-F and ITS055-R (Marin et al., 1998). Polymerase chain reactions (PCRs) contained 100 ng template DNA, 1 × PCR Buffer (500 mM KCL and 100 mM Tris–HCl, pH 8.3), 2 mM $MgCl_2$, 0.8 mM dNTPs, 0.5 µM of each primer, 0.25 U of AmpliTaq DNA Polymerase (Applied Biosystems Inc., Foster City, CA, USA) and 14.5 µl sterile deionized water to reach a final volume of 25 µL.

Hot start PCR amplifications were performed using an Applied Biosystems GeneAmp PCR system (Applied Biosystems Inc., Foster City, CA, USA) as follows: 94 °C for 4 min; then 40 cycles of 94 °C for 30 s, 57 °C for 45 s, 72 °C for 2 min, and a final extension of 72 °C for 10 min. PCR amplification products were visualized by electrophoresis on a 1% TAE agarose gel adjacent to a 100 bp DNA ladder. Positive PCR products were purified using the Qiagen MinElute PCR purification kit (Valencia, CA, USA) following the manufacturer's instructions, and stored at -20 °C.

DNA sequencing was performed using ABI BigDye version 3.0; reactions consisted of 1.0 µl BigDye 0.5 µM forward or reverse PCR primer, 0.1 µl DMSO and 1-3 µl purified PCR product (adjusted according to concentration), which were brought to a total volume of 6 µl with nuclease-free water. Thermocycling conditions consisted of 60 cycles of 96 °C for 15 s, 50 °C for 5 s and 60 °C for 4 min. Reactions were precipitated using isopropanol, air dried, and resuspended in Hi-Di Formamide before being analyzed on an ABI 3730x1 capillary sequencer. Products were sequenced in both the forward and reverse direction.

2.4 DNA sequence analysis

To examine the phylogenetic affinities of *Pseudo-nitzschia* isolates from the GOM region, two separate analyses were carried out. The first examined LSU rRNA sequences from the full dataset, while the second examined a subset of the ITS2 sequences to resolve phylogenetic affinities of *P. pseudodelicatissima* complex isolates. The isolates and corresponding GenBank sequence accession numbers used in this study are listed in Table S2.

Sequences were manually edited and assembled using Sequencher 4.9 (Gene Codes, Ann Arbor, MI, USA). Consensus sequences were aligned with rRNA gene sequences available

in GenBank using the ClustalW (Thompson et al., 1994) and the alignment refined using MUSCLE (Edgar, 2004), as implemented in bioinformatics software Geneious Pro 5.5.6 (Biomatters, Auckland, NZ), and subsequently inspected by eye. The LSU alignment included 41 taxa and 594 positions, and the ITS2 alignment included 26 taxa and 375 positions.

Modeltest V. 3.7 (Posada and Crandall, 1998) was used to select the appropriate model of nucleotide substitution for phylogenetic analyses. Phylogenetic trees were constructed with PAUP* version 4.0b 10 (Swofford, 2000), using neighbor joining (NJ), maximum parsimony (MP) and maximum likelihood (ML) analyses. *Fragilariopsis curta* strain 1-A (Genbank accession number AF417659) was used as an outgroup in the LSU dataset, and *P. pungens* var. *pungens* (regional strain Pn158-07A6; KF006830), identified during the current study, was used as an outgroup in the ITS2 dataset. Parsimony analyses were conducted using the heuristic search, simple addition, with gaps treated as missing data. For the LSU and ITS2 datasets, heuristic searches employed the TVM+I+G and TVM+G evolutionary models, respectively, as recommended by the Akaike Information Criterion in Modeltest (AIC). Bootstrap support values were determined for NJ, ML and MP using 100 replicates.

2.5 Analysis of rDNA secondary structure

To further consider the genetic relatedness of the eight sequenced isolates identified as *P*. sp. GOM to closely related taxa, a comparison of the secondary structures of the ITS2 rDNA sequences was conducted to assess structural differences and identify compensatory base pair changes (CBCs) and hemi-CBCs (see Coleman, 2003). For these analyses, ITS2 secondary structures for *P*. sp. GOM were generated using Mfold software (Zuker, 2003), with formation of major structural motifs common to different *Pseudo-nitzschia* species imposed as constraints during folding. ITS2 secondary structure of *P*. sp. GOM was compared with the secondary structure of strains Ner-D6 (*Pseudo-nitzschia* sp.; Orive et al. 2010) and Hobart5 (*Pseudo-nitzschia* sp.; Lundholm et al. 2003), and of strains Al-15 (*P. pseudodelicatissima*) and AL-17 (*P. cuspidata*) predicted by Amato et al. (2007). Diagrams of the RNA structures were created using the program VARNA 3.1 (Darty et al., 2009), and helices labeled according to Mai and Coleman (1997).

2.6 Toxin analyses

Forty-six isolates (Table S1), representing seven of the nine species identified in the GOM region (Table 1), were grown in nutrient-replete batch culture and screened by Biosense ASP ELISA (Amnesic Shellfish Poison, enzyme-linked immunosorbent assay) for the production of DA, expressed as ng DA ml^{-1} (intracellular + extracellular DA). Two species, *P. americana* and *P. heimii*, were excluded from all toxin analyses as they did not persist in culture long enough for testing. The most toxic isolates (n=15) were subsequently regrown and analyzed for DA by four methods: ELISA, LC-FLD after chemical derivatization with 9-fluorenylmethylchloroformate (FMOC-LC-FLD), LC-MS or LC-UVD. In the latter comparative analyses (Table 4), toxin concentrations, expressed as “toxin per cell in culture”, were measured as total extracellular plus intracellular DA divided by the number of

cells present at culture harvesting, because cells were not separated from the growth medium prior to extraction.

ELISA screening—In preparation for ELISA screening, multiple isolates of seven *Pseudo-nitzschia* species (*P. seriata*, 5 isolates; *P*. sp. GOM, 10 isolates; *P. subpacifica*, 4 isolates; *P. pungens*, 5 isolates; *P*. turgidula, 8 isolates; *P. fraudulenta*, 2 isolates; *P. delicatissima*, 12 isolates; see Table S1) were inoculated from 50-ml stock culture flasks into 50-ml culture tubes containing 25 ml of f/2 medium and grown under batch-culture conditions as described above. Cultures were sub-sampled, 0.5 ml, for DA quantitation 17 days after inoculation, corresponding with early to middle stationary phase. For 22 of the isolates, additional sub-samples were collected on days 5 and 28 after inoculation, corresponding with exponential and late-stationary phase, respectively, to compare DA concentrations across different growth stages. Growth phase was determined by fluorometry (model AU-10, Turner Designs). Sub-samples were probe-sonicated (Branson Sonifier 250, Branson Ultrasonic Co., Danbury, CT, USA) for 40 s, on ice, to disrupt the cells and then 0.22 μl was filtered (Millex-GV, Durapore PVDF, Millipore, Bedford, MA, USA) to remove cell debris before analysis. The filtrate was analyzed using the Biosense amnesic shellfish poison (ASP) ELISA test kit (Biosense, Norway). Assays were performed as per the manufacturer's specifications, using a standard microplate absorbance reader at 450 nm; the assay had a limit of detection (LOD) of 0.011 ng DA ml^{-1}. While ELISA provided a range of toxicity for each of the seven species, it is important to note that screening results should be considered semi-quantitative as cell concentrations were not enumerated in the 46 cultures and fluorometry readings were not standardized; cultures grew to varying densities and degrees of health.

Comparative analyses: ELISA, FMOC-LC-FLD, LC-MS and LC-UVD—Isolates found to be moderately to highly toxic by ELISA screening, i.e. containing >1 ng DA ml^{-1}, were then re-inoculated into 50-ml culture tubes under the above conditions and sub-sampled for paired analysis by ELISA and FMOC-LC-FLD (Pocklington et al., 1990) using isocratic elution. Fifteen isolates were analyzed, representing four species: *P. seriata*, 5 isolates; *P. pungens*, 1 isolate; *P. subpacifica*, 1 isolate; and *P*. sp. GOM, 8 isolates. Two species, *P. delicatissima* and *P. fraudulenta*, were excluded from this phase of analyses as they contained low concentrations of DA during the ELISA screening, suggesting samples would be below the detection limit, 3 ng DA ml^{-1}, of the FMOC-LC-FLD method. DA was also analyzed in a subset of seven isolates by LC-MS (LOD = 0.15 ng DA ml^{-1}) and LC-UVD (LOD = 0.042 ng DA ml^{-1}) subsequent to the addition of trifluoroacetic acid (Caledon, Georgetown, Canada) at 0.15% (pH 2.2) and injection of large (100 μl) sample volume (Mafra et al., 2009). For all 15 isolates, sub-samples were harvested for DA analyses at early to middle stationary phase, as described for the preliminary screening. Concurrently, a sub-sample of each culture was collected and the cells were fixed with Lugol's solution and enumerated in a Sedgewick-Rafter chamber using a Nikon Labophot microscope at 100X to determine the number of cells extracted for DA. All toxin analyses were run within three months of extraction and extracts were frozen at -20 °C in the interim. Standard curves were achieved using certified reference material (Institute for Marine Biosciences, National Research Council, Halifax, Canada). For the comparative analyses (Table 4), results are

presented as toxin per cell in the whole culture (cells + medium; fg DA cell^{-1}), which was calculated by dividing the amount of DA in a 0.5-ml subsample of culture by the number of cells harvested for extraction. Regression analysis (Sigmaplot 12.0) tested for agreement between DA detection methods; alpha was set at 0.05 for statistical analyses.

2.6 Distribution of species in the Gulf of Maine

The qualitative species distribution data presented here describe the locations where the three most frequently observed species were isolated (representing 75 stations) and/or where these species were identified in field material (with EM, at 28 of the 75 stations where isolates were obtained).

3. Results

3.1 Species diversity

Nine *Pseudo-nitzschia* species were identified among isolates and in field samples collected from the GOM region during the 2007 and 2008 cruises: *P. americana, P. delicatissima, P. fraudulenta, P. heimii, P. pungens, P. seriata, P. subpacifica, P. turgidula* and a species within the *P. pseudodelicatissima* complex referred to as *P.* sp. GOM (to differentiate GOM regional strains from those isolated in other regions). Tables 2-3 and Appendix A summarize the morphological features used for differentiating *Pseudo-nitzschia* species occurring in the GOM region. Kaczmarska et al. (2005; 2007) divided *Pseudo-nitzschia* species in the BOF into three morphologically distinct groups to facilitate recognition during routine LM enumeration of phytoplankton. We similarly considered the transapical and apical axes as well as cell shape, and defined four size classes. The first group included short (<60 μm long), thin (<2.3 μm wide) cells that comprised the *P. delicatissima*/*P. pseudodelicatissima* complex. The "P. *seriata*" group consisted of *P. fraudulenta, P. subpacifica, P. seriata* and *P. heimii*. Cells were wide (>4.0 μm) and were symmetrical or asymmetrical depending on species. The "*P. pungens*" group included *P. pungens* and *P. turgidula*, which fell between these size classes with respect to transapical width (2.5-4.0 μm). *Pseudo-nitzschia multiseries* was not found in the present study, but based on previous regional records (e.g., Hargraves and Maranda, 2002), it would fit in this group as well. Cells in the fourth group, represented only by *P. americana* in our study, were solitary, small (length <26 μm, width <2.0 μm) and exhibited rounded apices compared to other species.

3.2 Taxonomic analyses

The specific morphological and genetic features associated with each species were classified using a combination of SEM, TEM and DNA sequencing. Morphospecies designations were confirmed through phylogenetic analyses and modified if necessary. Most of the isolates obtained conformed to previously published descriptions of species originating from regions including, but not limited to, the N. Atlantic (see detailed descriptions for each species in Appendix A); deviations were identified in only a subset of species and are further outlined below and/or in the supplemental material. For most isolates, LSU sequence data provided sufficient resolution for species identifications; however, ITS2 sequences were used to assess phylogenetic affinities of *P.* sp. GOM isolates, confirm the identification of *P.*

turgidula isolates, and to further support the classification of variants from the *P. pungens* and *P. delicatissima* groups.

In addition to confirming morphospecies identifications, phylogenetic analyses of LSU and ITS2 sequences highlighted genetic differentiation among regional species, including *P. subpacifica, P. turgidula, P. seriata, P. fraudulenta* and *P. pungens* var. *pungens*, and demonstrated that isolates were identical or nearly identical in sequence (>99% similar) to conspecific sequences selected from GenBank (Figs. 2, 3). Instraspecific sequence diversity was not detected in either LSU or ITS2 regions, and there was substantial concordance with respect to clade recovery among the tree topologies in ML, MP and NJ analyses. In analyses of both LSU and ITS2 sequences, regional *P. delicatissima* sequences clustered with GenBank sequences comprising clade A (cool waters), as defined by Kaczmarska et al. (2008). LSU and ITS2 sequences from *P*. sp. GOM were aligned with *P. cuspidata* and *P. pseudodelicatissima* sequences; a more in-depth consideration of this group is provided below.

Morphology of *Pseudo-nitzschia* sp. GOM—Fourteen isolates (Table S1) and cells in field material identified as *P*. sp. GOM were morphologically and genetically similar to species in the *P. pseudodelicatissima* complex, but were not readily assigned to any of these known species. Cells of *P*. sp. GOM form stepped colonies, generally consisting of 6-15 cells (and up to 30 in culture), overlapping by one-ninth of total valve length. Valves are linear or almost linear, gradually tapering towards the apices (Fig. 4A-E). Within some frustules, the separate apices varied slightly in shape, such that one end is more pointed and abruptly tapered, whereas the other end is more blunt and gradually tapered (Fig. 4A). The apical axis is 30-54 μm and the transapical axis is 1.5-2.1 μm. The raphe system is eccentric and is interrupted by a central nodule in the larger interspace between the central fibulae (Fig. 4F-G). The valve has 39-42 striae and 21-26 fibulae per 10 μm. Each stria contains one row of poroids, 5-6 in 1 μm; interstriae are narrower than the striae. Examination of poroid structure was possible for the subset of isolates (Table S1) examined with TEM. Poroids were divided into between four and eight irregular (with respect to shape, size and orientation) sectors (Fig. 4G-H); typically, variably sized sectors were scattered around the margin of the hymen, and sometimes clustered in close proximity to each other (Fig. 4H). The central velum is more often than not unperforated (Fig. 4). The pores within each sector vary in number and form unique patterns (Fig. 4F-H); within the same isolate, valves with larger or smaller sector sizes were observed. Terminal raphe fissures have a discrete helictoglossa. An approximately triangular terminal area is visible starting from the last fibula. Three bands constitute the cingulum (Fig. 4F, 4I). The valvocopula is composed of 52-56 rectangular striae (in 10 μm) with elongated poroids. Striae are two poroids wide and 2-3 poroids high. The first band has quadrangular striae; each stria is 2 poroids wide and 2 poroids high. In the second band the striae are simple, and are 2 poroids wide, one poroid high.

The majority of *P*. sp. GOM isolates resembled Pn236-07A2 and Pn202-07A8 (Fig. 4A-B), however additional morphological variability, especially in valve shape and poroid structure, was observed in *P*. sp. GOM strains Pn236-07A6 and En435-153-B5 (Fig. 4C-D).

Compared to other *P*. sp. GOM isolates (Fig. 4A-B), strain Pn236-07A6 (Fig. 4C) especially has narrower valves, and therefore, more pointed apices.

Pseudo-nitzschia sp. GOM shares an almost identical morphology (i.e., shape, morphometrics and poroid structure) with strain *P*. sp. Ner-D6, which was identified from the Bay of Biscay, Spain (Orive et al., 2010). Minor differences include slightly wider cells (up to 2.1 μm) and slightly fewer fibulae in some *P*. sp. GOM cells (Table 3). Isolates of *P*. sp GOM, especially strain En435-153-B5 (Fig. 4), are also morphologically similar to the Australian strain, *P*. sp. Hobart5 (Lundholm et al., 2003), in that both have a lanceolate valve shape, poroids split into perforated sectors that mostly cluster around the margin of the hymen, and similar numbers of sectors in the poroids. Strain En435-153-B5 has a higher density of fibulae (25 in 10 μm) relative to most other regional isolates and *P*. sp. Hobart5 (20-22 in 10 μm), and a wider valve (1.9-2.0 μm, compared to 1.4-1.6 urn for *P*. sp. Hobart5 and 1.5-2.1 for *P*. sp. GOM) (Table 3).

Phylogenetic inference and ITS2 secondary structure analysis for *Pseudo-nitzschia* sp. GOM—Sequences were generated for eight isolates of *P*. sp. GOM (Pn202-07A8, Pn202-07F1, En435-153B5, Pn236-07A4, Pn236-07A2, Pn236-07A3, Pn236-07F5, Pn237-07C5) and intraspecific variability was not detected for either the LSU or the ITS2. The morphologically aberrant strain En435-153B5 was confirmed to be *P*. sp. GOM, but Pn236-07A6 (Fig. 4C) was not successfully maintained in culture long enough to permit DNA-based analyses to confirm species identity. In both the LSU and ITS2 phylogenies, the GOM region *P. pseudodelicatissima* sequences clustered with *P. cuspidata* and *P. pseudodelicatissima* sequences from Lundholm et al. (2003), as well as additional sequences of those species from GenBank. This group, comprising the *P. pseudodelicatissima/cuspidata* species complex (Lundholm et al., 2003), was highly supported in all analyses (Figs. 2, 3). Phylogenetic analysis of ITS2 sequences supported the existence of three clades within this group (Fig. 3). The first clade comprised the *P*. sp. GOM strains, *P*. sp. Hobart5, and *P*. sp. Ner-D6, with strong bootstrap support (>90%). The second consisted of *P. cuspidata* isolates, which comprised a sister group to the first clade, with moderate bootstrap support. The third comprised the remaining *P. pseudodelicatissima* strains (AL-15, Tenerife8 and P11).

The ITS2 rDNA secondary structure of *P*. sp. GOM was compared with the most closely related strains in the ITS2 phylogeny, *P*. sp. Hobart5 and *P*. sp. Ner-D6 (Fig. 5A). Secondary structure comparisons were also made between *P*. sp. GOM and closely related species *P. pseudodelicatissima* (AL-15) and *P. cuspidata* (AL-17) (Fig. 5B). *Pseudo-nitzschia* sp. GOM was nearly identical to Ner-D-6, with the exception of two nucleotide changes: one base change (A/U→G/U) at position 134, which broke the pairing at that location, and the second (C→A) at position 298 (Fig. 5A). A deletion of two base pairs was also present at positions 298-299. More nucleotide changes were present in Hobart5 when compared to *P*. sp. GOM/Ner D-6. *Pseudo-nitzschia* sp. Hobart5 exhibited a different end loop composition and structure in helix I due to a 15 bp AT-rich insertion. One base change was present in helix 2 (U→G/U), as well as the base change at position 14 mentioned previously. In helix IV, two base changes were present (position 267: C→U; position; position 285; C→A), as well as two insertions, resulting in the formation of an internal loop

in the Hobart5 strain. Among *P*. sp. GOM, *P. pseudodelicatissima* (AL-15), and *P. cuspidata* (AL-17), the most notable structural difference was observed in the length and composition of helix 1, due to the aforementioned AT-rich insertion situated in the end loop of *P*. sp. GOM, *P*. sp. Ner D-6 and *P*. sp. Hobart5 (Fig. 5B). In helix 1 of AL-17, two base pair changes were present at positions 44-45 (G/C→G/U; U/A→U/G), both of which broke base pairings at those locations. In helix III, three hemi-compensatory base pair changes were observed: U/G→U/A at position 161 in AL-15, and U/G→U/A at positions 169 and 208 in AL-17. In both AL-15 and AL-17, a nucleotide substitution A→U at position 204 resulted in a differentiated bulge conformation at this location (Fig. 5B). Additional base pair substitutions were also observed at positions 43 and 46 (U→C; AL-17), and at position 48 (G→U; AL-15 and AL-17), the latter of which broke the base pairing. In helix IV, differences in end loop structure were observed as well as one compensatory base pair change at pairing 12 (A/U→G/C). A nucleotide substitution was also observed at position 275 (C→U) in AL-15 and AL-17. Finally, three base pair changes in the regions between helices were observed: G→A at position 59 in both AL-15 and Al-17; A→U at position 255 in AL-17; and A→G at position 256 in AL-15.

3.3 Domoic acid levels in the cultures

Seven of the nine species identified in the GOM region were screened by ELISA and found to produce DA in culture (Table 1). Concentrations in culture ranged from trace (<1 ng ml^{-1}), to highly toxic (>100 ng ml^{-1}), with variation found at both the strain and species levels despite similar growth conditions. Below are details of this semi-quantitative screening and subsequent comparative analysis by ELISA, FMOC-LC-FLD, LC-MS and LC-UVD. The latter three methods allowed for the structural confirmation of DA (i.e., LC-MS) and/or a comparison of the sensitive ELISA against robust and selective analytical methods.

ELISA screening—All 46 isolates of *Pseudo-nitzschia* tested positive for DA when screened by Biosense ASP ELISA (Table 1), with the majority (68%) producing very low levels of DA (≤1 ng ml^{-1}), and 15 isolates containing moderate to high concentrations of DA. Values ranged over three orders of magnitude (0.06–140 ng ml^{-1}) during early to middle stationary phase. The lowest concentration detected in culture, over all the growth stages, was approximately 4x higher (0.04 ng ml^{-1}) than the detection limit of this sensitive assay (0.011 ng ml^{-1}). *Pseudo-nitzschia seriata* and *P*. sp. GOM contained the highest concentrations and greatest range of DA of all species tested: *P. seriata* (5 isolates) ranged from 1.4 – 140 ng ml^{-1} and *P*. sp. GOM (10 isolates) ranged from 0.24 – 320 ng ml^{-1} (Table 1). Isolates of *P. subpacifica* (4 isolates) and *P. pungens* (5 isolates) contained 0.06 – 1.1 ng ml^{-1} and 0.04 – 1.1 ng ml^{-1}, respectively. The other three species screened for toxin production contained only trace levels of DA (Table 1): *P. turgidula* (8 isolates): 0.08 – 0.71 ng ml^{-1}; *P.fraudulenta* (2 isolates): 0.18 – 0.39 ng ml^{-1}; and *P. delicatissima* (12 isolates): 0.11 – 0.39 ng ml^{-1}.

During the ELISA screening, a subset of 22 isolates was also analyzed at multiple growth stages. In general, toxin concentrations for each species were greater during early to middle stationary phase than during exponential growth; toxin concentrations were either

maintained or decreased slightly by late stationary phase. Average concentrations of DA (0.1 – 0.7 ng ml^{-1}) in *P. delicatissima, P. pungens, P. subpacifica* and *P. turgidula* remained low across the growth stages, with values less than doubling as cultures transitioned to early-mid stationary phase. The average toxin concentrations of *P. seriata* isolates, however, increased an order of magnitude from exponential to early stationary phase (from 6.7 to 76 ng ml^{-1}), and remained high into late stationary phase (76 ng ml^{-1}). DA concentrations in isolates of *P*. sp. GOM remained relatively high across all growth stages, with concentrations averaging 64, 82, and 67 ng ml^{-1}, for exponential, early stationary and late stationary phases, respectively.

Comparative analyses: ELISA, FMOC-LC-FLD, LC-MS and LC-UVD—Of the initial 46 isolates initially screened by ELISA, the most toxic isolates (containing ≥1 ng DA ml^{-1}) were chosen to undergo additional paired analyses by ELISA and FMOC-LC-FLD. Of these 15 isolates (Table 4), seven were also analyzed by LC-MS and LC-UVD to further compare methodologies. DA was detected in all 15 isolates by ELISA during comparative analyses. DA was confirmed by LC-MS in *P*. sp. GOM; however, toxin levels in *P. pungens* (Pn295-07 B4) and *P. subpacifica* (Pn252-07 E7) were below the lower detection limit for LC-MS (0.15 ng ml^{-1}) and DA could not be structurally confirmed.

Domoic acid concentrations, as determined by ELISA and FMOC-LC-FLD, were in good quantitative agreement during paired analyses (Fig. 6A; r^2=0.868) and an excellent correlation was observed between DA concentrations quantified by ELISA and LC-MS (Fig. 6B; r^2=0.997) or LC-UVD (Fig. 6C; r^2=0.999). Isolates were excluded from statistical analyses when levels were below detection limits (Table 4; Pn236-07 A6, *P*. sp. GOM; Pn252-07 E7, *P. subpacifica*).

When DA concentrations were adjusted for the number of cells extracted, *P. seriata* was the most toxic species in our study, with some isolates producing up to 3,500 fg DA $cell^{-1}$ (Table 4). *Pseudo-nitzschia* sp. GOM was slightly less toxic (19 – 380 fg $cell^{-1}$). Only one isolate of *P. pungens* was analyzed during paired analyses, and it contained a very low level of DA (0.4 fg $cell^{-1}$). Toxin production levels for strains Pn236-07 A6 (*P*. sp. GOM) and Pn252-07 E7 (*P. subpacifica*) could not be calculated as no cells were detected in the sub-samples; ELISA determined that toxin concentrations were 0.24 ng ml^{-1} and 0.06 ng ml^{-1}, respectively. It is important to note that values are expressed as “toxin per cell in culture”, determined as total extracellular plus intracellular DA divided by the number of cells present at culture harvesting, because cells were not separated from the growth medium prior to extraction.

Seventy percent of the most toxic isolates appear to have exhibited a decrease in toxicity over time in culture. This was determined by directly comparing ELISA results between the initial screening and later quantitative analyses. Four to five months passed between the two inoculations and in both steps, culture was extracted when cells were in early to middle stationary phase. For most isolates, toxicity decreased by a factor of 5-15. However, in one strain of *P*. sp. GOM (Pn202-07 F1), toxicity decreased by a factor of 62, dropping from 37 to 0.6 ng DA ml^{-1}. This decrease is likely due to a reduction in toxin production per cell as

opposed to a decrease in culture cell density, as fluorescence measurements at the time of sampling were similar or greater in later cultures.

3.4 Species distribution in the Gulf of Maine

The spatial and temporal distribution of *Pseudo-nitzschia* species during our study was inferred either from EM-characterized field material or from successful isolations. Generally, *Pseudo-nitzschia* cells were detected throughout the study region (Fig. 7) as part of mixed phytoplankton assemblages, although *Pseudo-nitzschia* dominated assemblages at a few stations. For example, during the May 2008 cruise, a nearly monospecific bloom of *P. delicatissima* was observed in field material from Casco Bay (Fig. 7A). The majority of isolates obtained were identified as *P. delicatissima* (66 isolates) or *P. seriata* (26 isolates); fewer than 10 isolates each of *P. fraudulenta, P. heimii, P. pungens, P. subpacifica* and *P. turgidula* were isolated, and *P. americana* was only identified in field material.

The successful isolation of numerous *P. delicatissima* isolates during each cruise, from locations in nearshore, shelf and offshore waters, highlighted the pervasive presence of this species in the system; this species was present in at least 78% of samples collected (Fig 7A). In contrast, other species, including the more toxic species *P. seriata* and *P*. sp. GOM (Fig. 7B-C), appeared to have a more restricted spatial and/or temporal distribution. In addition to *P. delicatissima*, three other species were observed during all cruises: *P. fraudulenta, P. turgidula* and *P. seriata*. The distribution of *P. fraudulenta* and *P. turgidula*, based on only a small number of observations, also spanned nearshore and offshore waters; *P. fraudulenta* was apparently broadly dispersed through the system, and *P. turgidula* was found in the BOF and along the southern flank of Georges Bank. For *P. seriata*, most isolates were obtained from Georges Bank during the April/May and May/June cruises in 2008; only a single isolate was obtained from nearshore waters during those cruises. In contrast, during October 2007, *P. seriata* isolates were successfully obtained from offshore waters north of Georges Bank, and nearshore and shelf samples collected north of 42° N. Interestingly, the highest *Pseudo-nitzschia* species diversity, and the only observations of *P. subpacifica, P. americana* and *P*. sp. GOM, occurred during October 2007. One species, *P. americana*, was only identified in field material, and only at Wilkinson Basin and in Eel Pond, a shallow embayment located near Woods Hole, MA. In the Eel Pond samples, single cells of *P. americana* were epiphytic on other diatoms, including *Chaetoceros* sp., *Asterionellopsis glacialis* and *Bacteriastrum* sp. In contrast, *P. subpacifica* and *P*. sp. GOM were isolated from coastal samples (Wilkinson Basin and Georges Bank).

4. Discussion

Pseudo-nitzschia species were present throughout the GOM region during each of the October 2007, April/May 2008 and May/June 2008 survey cruises and in a small number of samples collected outside these cruise efforts (Table S1). *Pseudo-nitzschia* distributions extended north from Cape Cod to the BOF, Canada, and from nearshore estuarine-influenced systems (e.g., Casco Bay), to offshore regions, most notably, Georges Bank (Fig. 1). Two species, *P. delicatissima* and *P. seriata*, were most frequently isolated and observed in field material, corroborating some of the earliest studies that described the prevalence of these same species in the GOM region (e.g., Bigelow, 1926; Gran and Braarud, 1933;

Lillick, 1940). Early descriptions of these species used LM to define species based on gross morphology (in particular cell width). In addition to the eight *Pseudo-nitzschia* species observed in the present study (*P. americana, P. fraudulenta, P. subpacifica, P. heimii, P. pungens, P. seriata, P. delicatissima* and *P. turgidula*), an undescribed species, referred to here as *P*. sp. GOM, was established in culture and successfully differentiated from morphologically and genetically similar species within the *P. pseudodelicatissima* complex. Including *P*. sp. GOM, up to 14 *Pseudo-nitzschia* species are so far putatively identified in the GOM system: *P. americana, P. calliantha, P. cuspidata, P. delicatissima, P. fraudulenta, P. hasleana, P. heimii, P. multiseries, P. pseudodelicatissima, P. pungens, P. seriata, P. subpacifica, P. turgidula* and *P*. sp. GOM (Kaczmarska et al., 2005; Kaczmarska et al., 2007; Kaczmarska et al., 2008; Leandro et al., 2010; Lundholm et al., 2012). Sequences in GenBank for *P. subpacifica* and *P. heimii* are nearly identical (ITS1; Hubbard et al., 2008; Marchetti et al., 2008), and these two species were distinguished here based on morphological differences in valve size and the number of poroid rows in the valvocopula (Table 2), as sequence data were not obtained for isolates identified as *P. heimii*. It is possible that *P. subpacifica* and *P. heimii* actually represent the same species, although additional taxonomic effort is needed to substantiate this. The full extent to which descriptions of *P*. cf. *calliantha* (Leandro et al., 2010), *P*. sp. GOM (this study), *P. calliantha* (Kaczmarska et al., 2005; Lundholm et al., 2003), and *P. pseudodelicatissima* (Kaczmarska et al., 2005; Martin et al., 1990) refer to multiple species and/or populations in the GOM system is still not entirely resolved (see Table 3). Recently, Leandro et al. (2010) discriminated *P. pseudodelicatissima, P*. cf. *calliantha, P. cuspidata* and *P. hasleana* in the region, and occasionally observed assemblages comprised of multiple species in the *P. pseudodelicatissima* complex.

Our analyses recovered a phylogenetically and morphologically distinct group in the *P. pseudodelicatissima* complex, comprising the *P*. sp. GOM isolates, the Spanish isolate *P*. sp. Ner-D6, and the Australian isolate *P*. sp. Hobart5, which was also distinguished from other clades in our ITS2 structural analyses (Fig. 5). The novel group has several morphological characters that distinguish it from others in the *P. pseudodelicatissima* complex, including the number of striae in 10 μm, the features of striae in the valvocopula (number in 10 μm and rows of poroids), and the unique characteristics of the irregular poroid sectors (Table 3). Models of ITS2 secondary structure have been used to support species designation in the genus (Lundholm et al., 2012) and have been shown to accurately discriminate among biological species (i.e., reproductively isolated isolates) in *Pseudo-nitzschia* (Amato et al., 2007). Experiments by Amato et al. (2007) showed that mating was only successful for strains with identical ITS2 helix regions (lacking CBCs or HCBCs), and more importantly demonstrated reproductive isolation between two of the clades within the *P. pseudodelicatissima* complex: *P. pseudodelicatissima* and *P. cuspidata*. The separation of members of the *P. pseudodelicatissima* complex into phylogenetically distinct clades, the differences in ITS2 secondary structure among these clades, and the demonstrated correlation between ITS2 structure and sexual compatibility support the classification of *P*. sp. GOM and closely affiliated strains *P*. sp. Hobart and *P*. sp. Ner-D6 as a separate species, although reproductive compatibility among these variants and with other species in the *P. pseudodelicatissima* complex has not yet been tested. The morphological and genetic

variability among *P*. sp. GOM, *P*. sp. NerD6 and *P*. sp. Hobart strains, and the broad geographic range of these strains, suggests that there may be physiological differences within this group; to our knowledge, the toxicity quantified for *P*. sp. GOM is the first report among these isolates.

These results are congruent with, and extend, current taxonomic studies of the *P. pseudodelicatissima* complex (Amato and Montresor, 2008; Lundholm et al., 2012; 2003; Orive et al., 2010). At least eight known species comprise the complex: *P. caciantha, P. calliantha, P. circumpora, P. cuspidata, P. fryxelliana, P. hasleana, P. mannii* and *P. pseudodelicatissima* (Amato and Montresor, 2008; Lim et al., 2012; Lundholm et al., 2012; Lundholm et al., 2003). Although *P*. sp. GOM groups with *P. pseudodelicatissima* and *P. cuspidata* in phylogenetic analyses, morphologically, *P*. sp. GOM is clearly distinct from those species, and instead more closely resembles *P. fryxelliana, P. hasleana, P. mannii*, and *P. circumpora*. Of those species, *P. calliantha, P. hasleana, P. pseudodelicatissima*, and *P. cuspidata* have been identified in the GOM region (Lundholm et al., 2012; Leandro et al., 2010).

Pseudo-nitzschia pseudodelicatissima and P. cuspidata are readily differentiated from *P*. sp. GOM with respect to poroid structure and sector number (Table 3). Although the valvocopulae of the three species share similar ranges of striae numbers, *P. pseudodelicatissima* and *P. cuspidata* have only one poroid row (Lundholm et al., 2003; Moschandreou et al., 2010), whereas *P*. sp. GOM has two. Interestingly, Kaczmarska et al. (2005) reported high variability in valve poroid structure in cells from the BOF, and were able to distinguish three groups based on the number of sectors in the poroids, which varied from 2 to 6. Their types 1 and 2 (with 3-4 and 4-6 sectors, respectively) shared other similar features to *P*. sp. GOM (see Table 3 for comparison). In comparison to the original description of *P. calliantha* (Lundholm et al., 2003), *P*. sp. GOM exhibits fewer sectors in the poroids and more striae. However, Moschandreou et al. (2010) recorded *P. calliantha* cells with 35-42 striae in 10 μm, more similar to the range observed in *P*. sp. GOM. In the valvocopula, *P. calliantha* exhibits considerably fewer striae than *P*. sp. GOM, but more poroids. The recently described *P. hasleana* (Lundholm et al., 2012) shares overlapping morphometric traits with *P*. sp. GOM (Table 3), although some *P. hasleana* isolates are wider (up to 2.8 μm) compared to *P*. sp. GOM (up to 2.1 μm). Furthermore, *P. hasleana* generally exhibits fewer sectors in the poroids, has fewer fibulae in 10 μm, and the valvocopula is less striated in 10 μm than *P*. sp. GOM.

Both *P*. sp. GOM and *P. caciantha* share similar numbers of poroids and sectors (Table 3). However, larger sectors and wider valves and fewer striae and fibulae are associated with *P. caciantha* relative to *P*. sp. GOM. In *P*. sp. GOM, the valvocopula is also more densely striated, with fewer poroids per row (2-3 in *P*. sp. GOM and 3-5 in *P. caciantha). Pseudo-nitzschia mannii*, recently described by Amato and Montresor (2008), also closely resembles *P*. sp. GOM with respect to cell overlap, width and number of poroids and fibulae. In the valvocopula the main features differentiating *P. mannii* include fewer striae in 10 μm (46-48), an additional poroid row and fewer striae (Amato and Montresor, 2008). In the valve, the sectors in the poroids of *P. mannii* are larger than those in *P*. sp. GOM and therefore encompass a wider area of the poroids (see Amato and Montresor, 2008, p. 491,

Fig. 4; Moschandreou et al., 2010, p. 166, Fig. 25). *Pseudo-nitzschia circumpora*, recently identified in Bornean waters (Lim et al., 2012), has unique irregularly sized poroids, varying from round to elongated, in contrast to other species in the *P. pseudodelicatissima* complex. Most of its morphometric features are distinct from *P*. sp. GOM, particularly the number of striae (32-35 in 10 μm), poroids (1-4 in 1 μm) and fibulae (15-19 in 10 μm) (Table 3). The valvocopula of *P*. sp. GOM is more densely striated (52-56 in 10 μm) compared to *P. circumpora* (40-42 in 10 μm).

Taxonomy in this species complex is challenging and is still clearly under revision, both globally and in the GOM region (Lim et al., 2012; Lundholm et al., 2012; this study), and the morphological and genetic data provided for *P*. sp. GOM highlight important discriminating identification features to aid in future species classifications. In this and prior studies, the size, number and orientation of sectors dividing the poroid hymens for cells in the *P. pseudodelicatissima* complex can vary within the same valve and among valves of the same isolate (although these are also discriminating features of certain species), and across different strains of the same species (Kaczmarska et al., 2005; Lundholm et al., 2003). Discrimination of *P*. sp. GOM is greatly facilitated by examining sector characteristics with TEM and/or through using molecular methods that can discriminate cryptic and pseudo-cryptic species diversity. While there have been successes in the development of molecular probes for recognition of toxic *Pseudo-nitzschia* species (Cho et al., 2001; Scholin et al., 1996), probes that can distinguish species in morphologically and/or genetically similar complexes have proven more challenging to design (Barra et al., 2012; Smith et al., 2012), especially as the number of species in these taxonomically complex groups continues to grow. Genus-specific approaches such as Automated Ribosomal Intergenic Spacer Analysis (ARISA; Hubbard et. al., 2008) and environmental sequencing (McDonald et al., 2007) may facilitate routine identification of the numerous species in the *P. pseudodelicatissima* complex present in the GOM region.

Each of the regional *Pseudo-nitzschia* isolates tested here, representing seven of the nine species identified, was determined to be toxic using one or more quantitation methods (Tables 1, 4). Toxin concentrations measured by LC and ELISA were positively and significantly correlated, and we therefore conclude that the ELISA method was both reliable and sensitive. The lower detection limit of the ELISA permitted quantification of toxicity in isolates that were found to be non-toxic with LC methods, although for the two most toxic isolates, higher concentrations were predicted with ELISA relative to FMOC-LC-FLD (Table 4).

In culture, higher levels of DA toxicity are commonly, but not always, associated with *Pseudo-nitzschia* cells in stationary phase (Lelong et al., 2013). Correspondingly, regional isolates were harvested for toxin analysis once stationary phase was reached, to target a window when cells were most likely to be toxic. It should be noted that DA in our study was measured for isolates grown in replete f/2 medium, compared to other studies that either measure DA in the field during a toxic event, or manipulate DA production through specific nutrient speciation, limitation or starvation (Lelong et al., 2012; Trainer et al., 2012). The nutrient(s) limiting growth in our cultures was not determined, but was most likely Si (Bates et al., 1991). For the seven species screened with ELISA, toxicity (ng DA ml^{-1}) was

estimated to vary across five orders of magnitude among species (0.04 to 320 ng ml^{-1} for *P. pungens* and *P*. sp. GOM isolates, respectively) and up to four orders among isolates of the same species (e.g. 0.24 – 320 ng ml^{-1} for *P*. sp. GOM) (Table 1). Two species, *P. seriata* and *P*. sp. GOM, produced levels of toxin that are comparable to those species and/or strains implicated in toxic events outside of the GOM region, although variability in toxicity was observed across different isolates of both species. The most toxic isolate, a *P. seriata* strain, produced 3500 fg DA $cell^{-1}$, comparable to levels (80-7000 fg DA $cell^{-1}$) produced by *P. seriata* strains isolated during shellfish closures in the Gulf of St. Lawrence and the St. Lawrence Estuary (Couture et al., 2001; Trainer et al., 2012), but considerably less DA than isolates from Denmark (3.4×10^4 fg DA $cell^{-1}$) and Scotland (1.5×10^4 fg DA $cell^{-1}$). Isolates of *P*. sp. GOM varied in toxicity, from 20-400 fg DA $cell^{-1}$, and on average produced more toxin than a strain identified as *P. pseudodelicatissima* isolated from the BOF during a bloom (98 fg DA $cell^{-1}$; Martin et al., 1990). The maximum levels of cellular DA reported for *P. calliantha, P. pseudodelicatissima* and *P. cuspidata* in culture, regardless of geographic origin, are comparable to or less than those observed here in the least toxic isolates of *P*. sp. GOM (Trainer et al., 2012). Isolates of *P. delicatissima, P. fraudulenta, P. subpacifica, P. turgidula* and *P. pungens*, and some isolates of *P. seriata* and *P*. sp. GOM, produced low levels of DA. To our knowledge, this is the first report of toxicity for *P. subpacifica*, and for Atlantic isolates confirmed as *P. pungens* var. *pungens*. More studies than not have shown *P. pungens, P. delicatissima* and *P. fraudulenta* isolates not to produce detectable levels of DA. For *P. delicatissima*, at least, this may in part due to the presence of cryptic and pseudo-cryptic species, whose taxonomy has been under revision (Trainer et al., 2012); based on sequence data, the temperate form of *P. delicatissima* identified in the GOM region, largely in the BOF, is also present in the northeast Pacific, Denmark, and Portugal (see Appendix A). It is not known whether species identified in previous regional studies, including *P. cuspidata* and *P. hasleana*, are similarly toxigenic, although toxic isolates and toxic blooms of *P. cuspidata* have resulted in harvest closures in Washington State (Trainer et al., 2012) and toxin was detected but was below limit of quantification for one Washington isolate of *P. hasleana* (Lundholm et al., 2012). Intraspecific variability may also be important for toxicity (Evans et al., 2004); three *P. seriata* strains isolated from off the New Hampshire coast during the same cruise produced different amounts of DA in culture (Table 4, Table S1), although intraspecific taxonomic differentiation was not detected in either of the genetic markers (ITS2 and LSU) examined here. Intraspecific variability in toxin production has been observed in other *Pseudo-nitzschia* species, and can potentially be influenced by microbial diversity and abundance, timing in sexual reproductive cycles, as well as physiological factors apparently inherent to distinct isolates (Amato et al., 2010; Evans et al., 2004; Holtermann et al., 2010).

In order to evaluate the potential risk to human health from the neurotoxin DA in the GOM region, we considered our data in terms of both historical and contemporary reports of DA in the GOM and nearby systems along the N. American coast (Table 5). Most of the closures in eastern Canadian waters occurred during late summer to fall months and were restricted to a particular location. For example, ASP closures in PEI waters occurred during 1987-1989, 1991, 1992, 1994, 2000 and 2001 (Bates, 2004). The organism associated with these closures was *P. multiseries*. High DA levels in BOF shellfish during 1988 and 1995,

however, were instead linked to blooms of over 10^6 cells l^{-1} of *P. pseudodelicatissima*, subsequently described as *P. calliantha* (Lundholm et al., 2003), although this identification has since been questioned (Lundholm et al., 2012). In April 2002, the first ever spring ASP closure spanned most of the southern Gulf of St. Lawrence, necessitating regulation by multiple provinces (Table 5). Toxicity in the 2002 event was attributed to *P. seriata*, which reached concentrations exceeding 4×10^4 cells l^{-1} (Bates, 2004). In the Quebec waters of the Magdalen Islands (Gulf of St. Lawrence), smaller, more isolated blooms of *P. seriata* occurred in the two years preceding these events, primarily during June-July, when high levels of DA contamination were observed in the digestive glands of scallops (Couture et al., 2001). No additional closures have occurred in that region since the 2002 event, and Kaczmarska et al. (2005) noted that *P. multiseries* was not detected in the BOF after 2003. The latest closures in Canadian waters occurred recently in 2008, when harvests for scallops were closed in Quebec waters during July and August, and harvests for multiple shellfish species were closed for 10 days in the BOF, starting on August 29, 2008; the BOF closure extended to the U.S. border (Table 5).

Historically, DA testing in the GOM region has been conducted sporadically, and there are limited reports of DA levels in shellfish (Table 5). Commonly harvested molluscan bivalves in the GOM include soft-shell clams (*Mya arenaria*), blue mussels (*Mytilus edulis*), quahogs (*Mercenaria mercenaria*), ocean quahogs (*Artica islandia*), oysters (*Crassostrea virginica*) and sea scallops (*Placopecten magellanicus*) (Anderson et al., 2004), and blue mussels are commonly used as the sentinel species for biotoxin monitoring. The highest reported DA levels in the GOM were measured in scallops collected at Georges Bank (~1,300 μg DA g^{-1} digestive gland) and Browns Bank (~4,300 μg DA g^{-1} digestive gland) in April and May, 1995 (see Douglas et al., 1997). Notably, 4,300 μg DA g^{-1} represents one of the highest levels observed in any shellfish species worldwide (James et al., 2005; Picot et al., 2011; Van Egmond et al., 2004) and is comparable to levels observed in PEI scallops (4,180 μg DA g^{-1}) sampled in December 1987, following the first PEI ASP event, which included human fatalities (Haya et al., 1991). Relative to other shellfish species, scallops have demonstrated relatively slow accumulation and depuration rates and tend to become and stay more toxic than clams or mussels collected from the same area (Couture et al., 2001; Stewart et al., 1998; Wohlgeschaffen et al., 1992). High DA levels in the digestive gland, however, are not necessarily indicative of human risk; the European Union allows the harvesting of scallops when DA concentrations in the adductor muscle and the gonad remain below 4.6 μg DA g^{-1} (see Bogan et al., 2006), since DA accumulates primarily in the digestive gland, with only trace levels typically found in the adductor muscle (Couture et al., 2001; Douglas et al., 1997). Months after DA was detected in shellfish from the Browns and Georges Banks, a toxic bloom attributed to *P. pseudodelicatissima* closed shellfish harvests in the BOF during August, with DA levels in mussels reaching >60 μg DA g^{-1} (Martin et al., 2004). Nearly a decade later, DA was detected in whale tissue samples taken during a mortality event in 2003, on eastern Georges Bank (http://www.nefsc.noaa.gov/press_release/2003/news03.15.html). Sampling of 192 scallops collected from Georges Bank in 2004-2006 in a separate study found low levels of DA in each scallop, with the highest values near 10 μg DA g^{-1} soft tissue, excluding the gonads and the adductor muscle, which were measured separately and were less toxic. The most toxic scallops were collected along the southern

flank of the Bank (Day et al., 2007). A subsequent study found low DA levels in the majority of zooplankton samples and North Atlantic right whale (*Eubalaena glacialis*) fecal samples collected throughout the GOM during 2005-2006, although concurrently observed *Pseudo-nitzschia* cell concentrations remained below 10^4 cells l^{-1} (Leandro et al., 2010). Recently, the successful merging of volunteer networks with state and federal agencies identified potentially hazardous levels of *Pseudo-nitzschia* cells (>10^6 cells l^{-1}) in Maine coastal waters during July 2012, and resulted in the first ASP closure in New England waters (Table 5), although DA levels were subsequently determined to be below 20 μg DA g^{-1} and the closure quickly lifted. To date, this represents the only ASP closure in GOM waters, other than in the BOF.

The distribution and toxicity of the strains isolated in our study, along with these historical observations, provides preliminary insight into when and where toxic *Pseudo-nitzschia* blooms have the potential to occur in the GOM region. *Pseudo-nitzschia seriata* was observed in our study during all three seasons and was especially prevalent at certain Georges Bank locations during the spring and early summer cruises. In contrast, Atlantic and Pacific strains of *P. seriata* are genetically distinct and can be discriminated by a single polymorphic site in the ITS1 region (Hubbard et al., 2008), although toxicity has not yet been determined for Pacific strains. In contrast, *P*. sp. GOM was isolated during September and October only. The temporal occurrence of the two most toxic species corresponds well with the general toxicity patterns observed in nearby northern waters: *P. seriata* blooms in the late spring and early summer (in the Gulf of St. Lawrence) and *P. pseudodelicatissima* blooms in the late summer and fall (in the BOF) (Table 5). The detection of the two most toxic species, *P. seriata* and *P*. sp. GOM, during the October cruise, but only *P. seriata* during the spring and summer cruises, suggests that changes in species diversity that occur across seasonal time scales are likely to impact the timing and magnitude of DA toxicity. Some eastern Atlantic *P. seriata* isolates are able to maintain high growth rates in culture at 15 °C (Fehling et al., 2005; Fehling et al., 2004), wheras other isolates of this cold tolerant species demonstrate an inverse relationship between growth rate and temperature (Hansen et al., 2011; Lundholm et al., 1994). It is possible that a single *P. seriata* population persists in the greater GOM system from spring to fall (or longer), or that genetically, and potentially physiologically, distinct populations vary over space and time.

The detection of isolates of *P. delicatissima, P. fraudulenta, P. subpacifica, P. turgidula, P. pungens, P. seriata* and *P*. sp. GOM that produced low levels of DA in culture, and the broad temporal and/or spatial occurrence of *Pseudo-nitzschia* species in the system (this study, Leandro et al., 2010) is perhaps consistent with the observation of low but nearly ubiquitous levels of DA observed in GOM scallops (Day et al., 2007), copepods, krill and fecal material from whales (Leandro et al., 2010).

The apparent disappearance of *P. multiseries* from the GOM and nearby systems is curious; a similar trend was observed during the 1990s in European waters (Hasle et al., 1996; Lundholm et al. 2010). In the GOM, the timing corresponds well with the general decline in toxic closures north of the BOF, and suggests that *Pseudo-nitzschia* species composition plays an important role in patterns of DA toxicity spanning multi-decadal time scales, as well as event, seasonal and annual time scales (Hasle et al., 1996; Lundholm et al., 2010).

Seasonal variability in cyclonic and anticyclonic gyres in the GOM region influence the transport and distribution of planktonic species (Hannah et al., 1997; Li et al., 2011). It is interesting to consider whether these circulation features contribute to the development and transport of *Pseudo-nitzschia* blooms, including those that led to the high levels of DA observed in shellfish in 1995. For example, both Georges Bank and Browns Bank have recirculation features that contribute to enhanced biomass there. The partial gyre at Browns Bank is persistent across interseasonal time scales (Hannah et al., 2001), whereas recirculation intensifies typically throughout the summer at Georges Bank and weakens during winter months (McGillicuddy et al., this issue; Townsend et al., 2010b). Along the west coast of the U.S., *Pseudo-nitzschia* species are sometimes associated with offshore retentive features such as the Juan de Fuca Eddy and Heceta Bank, and under certain wind conditions, these blooms can be advected onshore where they represent a greater threat to human health (Pitcher et al., 2010; Trainer et al., 2008). It is not yet clear whether the offshore retentive features in the GOM are an analogous potential source of toxic *Pseudo-nitzschia* cells in nearshore regions, although physical interactions between gyres can sometime result in enhanced cross-shelf transport in the GOM, opening up dispersal pathways for plankton (Hannah et al., 1997).

Additional sampling is warranted to more fully determine the spatial and temporal extent and severity of toxic *Pseudo-nitzschia* blooms and DA-contaminated shellfish in the GOM region. Nevertheless, several important lines of evidence suggest that DA has the potential to occur there at concentrations that could have detrimental consequences for ecosystem and wildlife health: (1) high DA levels observed in GOM scallops during spring 1995; (2) *Pseudo-nitzschia* blooms in late summer in the GOM, sometimes resulting in DA closures (Table 5, Martin et al., 1990; Martin et al., 2004); (3) low levels of DA found in nearly every sample collected during regional sampling efforts spanning multiple seasons and years (Day et al., 2007; Leandro et al., 2010); (4) the presence of at least seven toxic *Pseudo-nitzschia* species in the system (Martin et al., 1990; Villareal et al., 1994; this study); and (5) the broad temporal window when these toxic species were observed (Leandro et al., 2010; this study).

Toxic *Alexandrium* spp. have the potential to co-exist with toxic *Pseudo-nitzschia* spp. in time and/or space in the GOM region (Gettings et al., submitted, Martin et al., 2004; this study). Shellfish in the GOM frequently accumulate high levels of PSP toxins that require regulation, however the effects of concurrent exposure to neurotoxic PSP and ASP toxins have not yet been investigated. In contrast to the ASP symptoms associated with acute DA exposure, chronic (long-term, low-level) exposure to DA has been found to cause a unique toxicosis in naturally exposed sea lions (Goldstein et al., 2008), and induced an antibody response and increased neurologic sensitivity to the toxin in subsequent exposures in a vertebrate model (Lefebvre et al., 2012). As such, chronic low-level exposure to DA, and the synergistic or additive effects with exposure to co-occurring ASP and PSP toxins, requires further investigation to better assess human and wildlife health risks and the implications for the management of nearshore and offshore shellfish resources.

5. Conclusions

This work provides a comprehensive taxonomic characterization of *Pseudo-nitzschia* spp. in the GOM region, including the identification of seven DA-producing species. Comparisons of various analytical techniques demonstrated that the ELISA method for DA quantification is a reliable method compared to more complex and expensive analytical methodologies typically used to assay DA in seawater, phytoplankton, and shellfish samples, although this method has not been approved by the National Shellfish Sanitation Program for regulatory applications. Our toxicological data demonstrate that the GOM region harbors multiple DA-producing *Pseudo-nitzschia* species, and this characterization of regional *Pseudo-nitzschia* species diversity is an important step towards developing tools and the fundamental knowledge needed to identify and respond to future blooms in the region. Using only LM, many of the highly and minimally toxic species cannot be distinguished, and in some cases, even EM was not sufficient for regional species identification.

The fundamental knowledge and outputs from this work will foster continued studies to further define the links among *Pseudo-nitzschia* species, DA production and environmental variability. Ultimately, these data will contribute to our understanding of the environmental drivers underlying the distribution of these species in the GOM region, including the identification of “hot spots” of toxicity. Martin et al. (1990; 2004) reported high levels of DA toxicity in BOF shellfish typically when cellular abundances of *P. pseudodelicatissima* approach 10^6 cells 1^{-1}. In comparison, high DA levels have been observed during toxic blooms of *P. seriata*, at 10^4-10^5 cells l^{-1} (Couture et al., 2001). Enumeration of *Pseudo-nitzschia* spp. in different LM classes is important for early detection, although critical levels are likely to be different for at least the two most toxic species identified here, based on the differences in toxin per cell associated with *P. seriata* and *P.* sp. GOM. As researchers, management and monitoring agencies continue to characterize the toxicity, frequency and magnitude of *Pseudo-nitzschia* blooms in the GOM, it may be necessary to adopt more extensive programs for monitoring DA levels in shellfish and for detecting toxic *Pseudo-nitzschia* species, similar to the PSP toxin monitoring program already established in the region.

Supplementary Material

Refer to Web version on PubMed Central for supplementary material.

Acknowledgments

The authors gratefully acknowledge the hard work of Bruce Keafer and Kerry Norton, along with many others, on obtaining the samples used in this study. We also thank two anonymous reviewers for their helpful comments and revisions. This work was supported by NOAA OHHI grant NA05NOS4781245, the ECOHAB grant program through NOAA Grant NA06NOS4780245, the Woods Hole Center for Oceans and Human Health through NSF grants OCE-0430724, OCE-0911031, and OCE-1314642, and NIH grants 1 P50 ES012742-01 and 1P01ES021923-01. Additional offshore samples were collected on several NOAA/NMFS cruises for the Woods Hole Center for Oceans and Human Health. A postdoctoral fellowship for L.F.F was provided by the Brazilian Research Council (CNPq - Contract n. 200243/2007-1) and the Organization of American States (OAS academic scholarship n. 20070456). A postdoctoral fellowship for K.A.H. was funded by the Woods Hole Oceanographic Institution. This is ECOHAB contribution number ECO756.

Appendix A: Taxonomic descriptions of Gulf of Maine Pseudo-nitzschia species

Detailed morphometric characteristics of GOM *Pseudo-nitzschia* species are included here as an appendix to augment existing descriptions for the region and to facilitate comparison of GOM isolates to *Pseudo-nitzschia* species from other regions.

Pseudo-nitzschia americana (Hasle) G. A. Fryxell *in* Hasle, 1993 (Fig. Al, A-D)

Isolates of *P. americana* from the GOM did not differ morphologically from the published ranges for *P. americana* (Hasle) Fryxell (Kaczmarska et al., 2005; Lundholm et al., 2002) and compared to other species, *P. americana* cells are more rectangular in girdle view. *P. americana* was solitary when observed in field material as epiphytes on the setae of *Chaetoceros*, *Bacteriastrum* and *Asterionelopsis glacialis* (Castracane) Round (cf. Lelong et al., 2012). Valves are slightly lanceolate with bluntly rounded apices, and some specimens exhibited one linear and one convex side (Fig. Al A-D). Two rows of small poroids are located close to the margin of the interstriae, and the strongly eccentric raphe system is located at the margin. The raphe is single branched, having fissures with discrete helictoglossa. Three bands were observed composing the cingulum. As GOM *P. americana* was not established in culture, this species was identified solely from morphological characteristics of cells observed in field samples.

Pseudo-nitzschia delicatissima. (Cleve) Heiden in Heiden et Kolbe, 1928 (Fig. Al, E-I)

The species composing the "*delicatissima*" species complex thus far include *P. arenysensis*, *P. decipiens*, *P. delicatissima*, *P. dolorosa* and *P. micropora* (cf. Lelong et al., 2012). We only observed *P. delicatissima* in the GOM. The features associated with GOM isolates of *P. delicatissima* are similar to prior descriptions of *P. delicatissima* cells from temperate waters, including the BOF (Trainer et al., 2012). Cells of *P. delicatissima* from the GOM were solitary in most of the cultures; a few had short stepped chains of 2-4 cells. In field material, *P. delicatissima* was commonly associated with *Phaeocystis* colonies. Valves are lanceolate, tapering towards the apices, with most cells exhibiting bilateral symmetry (Fig. Al E-I). The striae are composed of 2 rows of small poroids arranged in a variable pattern. The eccentric raphe system has two branches separated by a central nodule. A small helictoglossa appears in the terminal fissure. The fibulae are variably spaced along the raphe, leaving a large central interspace. Three bands constitute the cingulum. The valvocopula is perforated by one single longitudinal row of poroids, each one further divided in 3-4 sectors. The second band has one row of undivided poroids. In the LSU phylogeny, GOM isolates were most closely affiliated with the *P. delicatissima* clade 2 identified by Orsini et al. (2004), supported by moderate bootstrap values (Fig. 2). Analysis of ITS2 sequences was also carried out to further assess the phylogenetic affinities of GOM *P. delicatissima* isolates. *P. delicatissima* GOM sequences were 100% identical to ITS types from the North Atlantic comprising clade A (cool waters) defined by Kaczmarska et al.

(2008). These sequences were also clustered in the ITS2 phylogeny, with strong bootstrap support (Fig. 3).

Pseudo-nitzschia fraudulenta (P. T. Cleve) Hasle, 1993 (Fig. A2, A-F)

Cells of *P. fraudulenta* from the GOM were similar to those described elsewhere (e.g. Hasle et al., 1996; Fryxell and Hasle, 2003; Kaczmarska et al., 2005; Moschandreou and Nikolaidis, 2010) and are lanceolate with acute apices, are either symmetrical or slightly asymmetrical, with the raphe side being less convex than the distal side (Fig. A2A-F). The valvar surface is striated. Each stria is composed 2-3 rows of poroids. Interstriae are continuous with the raphe fibulae in most of the valve. The mantle is two poroids wide and 1-2 poroids high. The raphe system has two branches. At the central nodule, a larger interspace is evident, about 3.5 to 4 striae wide. Fibulae are equally spaced. A helictoglossa appears at each apex, surrounded by a small depression in part of the terminal area. Typically, an additional stria and 1 -2 isolated poroids occupy part of the terminal area at one apex, but not at the other. The cingulum contains four bands, all of them with acute apices. The valvocopula has rectangular striae, each one 2-3 poroids wide and 8-12 poroids high, measured in the central part of the valve. The striae gradually diminish in size toward the apices until completely disappearing. The second band is quadrangular, 2 poroids wide and 2 poroids high. The remaining two bands lack any ornamentation. Species designations based on morphological characters were supported by DNA sequence data from the GOM isolates, which were highly affiliated with *P. fraudulenta* sequences in GenBank (≥99.7% identity; LSU, ITS2), and clustered with *P. fraudulenta* GenBank sequences in the LSU phylogeny (Fig. 3).

Pseudo-nitzschia heimii Manguin, 1957 (Fig. A2, G-J)

Morphologically similar to *P. fraudulenta*, isolates of *P. heimii* displayed lanceolate valves with rounded apices that were slightly asymmetrical by having the proximal margin almost straight near the central region (Fig. A2, G-J). The material in our study agreed with the morphometric data recorded for *P. heimii* Manguin, 1957 (Almandoz et al., 2008; Hasle et al., 1996; Hasle, 1965; Hasle and Medlin, 1990) except for the number of striae in 10 μm, which was slightly higher than the recorded range (19-28 in 10 μm).

In general, the striae for *P. heimii* are wider than the interstriae. Each stria has two rows of poroids placed very close to the interstriae, hence leaving a long hyaline area between the two rows. Most of interstriae are displaced from the fibulae. The raphe system has two branches separated by a central nodule. Terminal fissures are slightly bent, reaching deeply into a large rectangular terminal area. A small helictoglossa surrounds the tip of each fissure. Fibulae are almost equally separated by interspaces, except for the two central ones, that are separated to form a large central interspace, about five striae long. Cingulum bands were not detected. GOM *Pseudo-nitzschia heimii* was not established in culture; therefore, this species was identified solely from morphological characteristics of cells observed in field samples.

Pseudo-nitzschia pungens var. *pungens* (Grunow ex Cleve) Hasle, 1993 (Fig. A3, A-G)

Three varieties of P. *pungens* have been well characterized in the literature: *P. pungens* var. *aveirensis*, *P. pungens* var. *cingulata* and *P. pungens* var. *pungens*. The material examined here conforms to *P. pungens* var. *pungens* (Fig. A3, A-G), although some GOM isolates exhibited a denser number of striae in the valvocopulae (15-23 in 10 μm) compared to prior descriptions (15-19 striae in 10 μm, after Hasle et al., 1995; Villac and Fryxell, 1998; Fernandes and Brandini, 2010). This feature of GOM *P. pungens* is shared with *P. pungens* var. *cingulata*, which has 20-24 striae in 10 μm in the valvocopula (Villac and Fryxell, 1998). However, the striae structure of the GOM isolates is identical to the nominal variety *Pseudo-nitzschia pungens* (Grunow ex Cleve) Hasle, 1993 Villac (var. *pungens*). Species designations of *P. pungens* var. *pungens* based on morphological characters were confirmed by DNA sequence data from the GOM isolates, which were identical to *P. pungens* var. *pungens* LSU and ITS2 sequences in GenBank.

Pseudo-nitzschia seriata. (Cleve) H. Peragallo in H. & M. Peragallo (Fig. A4, A-I)

For *P. seriata* from the GOM, morphometrics of valve and cingulum bands fall within the ranges attributed to specimens from other regions (Fig. A4, A-I). Only the apical axis of cultured cells appeared to be shorter than previous literature reports for *Pseudo-nitzschia seriata* (Cleve) H. Peragallo in H. & M. Peragallo (Fryxell and Hasle, 2003; Hasle et al., 1996; Hasle and Lundholm, 2005; Skov et al., 1999). Cells of *P. seriata* are lanceolate and asymmetrical with pointed apices in valve view. Cells generally were observed to have one convex side opposite a straight side, with the convex side only sometimes occurring on the same side as the raphe. The striae of the valve surface are composed of 3-4 rows of very small poroids. Those poroids in contact with the interstriae are larger than the poroids in the middle. At the apex, the last interstria is curved and bifurcated, occupying the terminal area that surrounds the raphe. The other apex has no further interstria development. The raphe system is highly eccentric, having one continuous fissure. Terminal fissures have a small but conspicuous helictoglossa. Fibulae are regularly spaced, leaving no central interspace, and the majority of fibulae are not aligned with the interstriae. The cingulum comprises three bands, all of them with acute apices. The valvocopula is wide; the striae in the central part are 2-3 poroids wide and 4-5 poroids high. The number of poroids gradually decreases toward the apices. The striae in the second band are two, rarely 3, poroids wide, and three poroids high. The third band is less structured, having 1-2 poroids per stria. Species designations of *P. seriata* based on morphological characters were confirmed by DNA sequence data from the GOM isolates, which were identical to *P. seriata* LSU and ITS2 sequences from GenBank.

Pseudo-nitzschia subpacifica. (Hasle) Hasle, 1993 (Fig. A5, A-E)

Isolates of *P. subpacifica* isolated from GOM samples were observed to have lanceolate valves with acute to subacute apices and although gross morphological characteristics such

as valve shape were consistent with published reports for this species, the specific morphometrics deviated somewhat. For example, the valve surface is striated (Fig. A5, A-E), and each stria has two rows of small poroids placed very close to the adjacent interstriae, similar to other *P. subpacifica*. The GOM isolates, however, exhibited narrower valves, fewer poroids (7-8 vs. 9-10 in 10 μm, Hasle and Syvertsen, 1997), and became more asymmetrical over time in culture. For *P. subpacifica*, the raphe system is double branched, having a central nodule that separates the branches. Terminal fissures have a small helictoglossa. Terminal area is triangular. Fibulae are unevenly spaced. Central interspace is conspicuous, 3-5 striae long. The cingulum is composed of three bands, all of them bearing pointed ends. The valvocopula is striated, each stria being two poroids wide and 4-5 poroids high (rarely 6) in the central region. The height of the striae gradually reduces toward their ends. The striae in the second band are two poroids wide and 2-3 poroids high, also reducing in size near the apex like the valvocopula. The third band lacks ornamentation. Species designations based on morphological characters were supported by LSU and ITS2 DNA sequence data from the GOM isolates, which were highly affiliated with *P. subpacifica* sequences in GenBank (99-100% identity). GOM and GenBank *P. subpacifica* sequences were also grouped in the LSU phylogeny, with nearly 100% bootstrap support (Fig. 2).

Pseudo-nitzschia turgidula (Hustedt) G. R. Hasle, 1993 (Fig. A6, A-I)

Cells of *P. turgidula* were identified in culture and field material; morphological variability and malformations (relative to previous descriptions; e.g. Hallegraeff et al., 2003) were observed more commonly within cultured cells. In general, cells are joined in stepped chains with overlap of one-fifth to one-sixth of the cell length (Fig. A6, A-I). Valves are linear with rounded apices, becoming lanceolate as the valves reduce through asexual division. In general the striae of the valvar surface are narrower than the interstriae and each generally consisted of two rows of small poroids. In some cells, striae near the center or the apices of the cell contained only a single row. In several valves the two rows of poroids appeared to have fused together producing a uniseriate stria whereas in others, poroids were missing. The raphe system is eccentric and composed of two branches separated by the central nodule. Terminal fissures are surrounded by a small helictoglossa. Terminal areas are triangular in shape. Fibulae are unevenly spaced and most of them do not align with interstriae. The central interspace is large and the central nodule is correspondingly conspicuous. The cingulum possesses three bands, the first two showing ornamentation, while the third is structureless. The valvocopula has 29-34 quadrangular striae, each 1 -2 poroids wide and 2-3 poroids high, gradually becoming smaller towards the ends of the cells, where the valvocopula lacks ornamentation. The second band has 34-36 striae in 10 μm, and is 1-2 poroids wide and one poroid high. Aberrant morphological features in cells examined from culture material included: a single raphe fissure in cells lacking a central nodule; larger interspaces in cells missing fibulae; and distorted cell shape. Some of the features associated with these cells made it difficult to definitively identify GOM isolates as *P. turgiduloides* or *P. turgidula* with EM, since valve width and the number of rows of poroids in the striae for GOM isolates were somewhat characteristic of both species. Common morphological traits among these two species include cell shape, the presence of a central nodule, a large central interspace and the number of poroids in 1 μm of the striae.

Cells of *P. turgiduloides* typically demonstrate 1-2 rows of poroids, compared to two rows of poroids for *P. turgidula*. Considering both field and culture materials, valves of GOM isolates exhibited 1-2 rows of poroids, more similar to that of *P. turgiduloides*; however, most valves from cultured material had two rows of poroids, more reflective of *P. turgidula*. Previous reports indicate that *P. turgidula* is generally wider (2.5-3.5 μm) than *P. turgiduloides* (1.2-2.7 μm), and there are more striae in the valves of *P. turgidula* relative to *P. turgiduloides* (23-28 compared to 18-24 striae in 10 μm; Hasle, 1965; Hasle and Syvertsen, 1997), although Ferrario et al. (2004) and Almandoz et al. (2008) recorded Antarctic specimens of *P. turgidula* with 17-24 striae. Material from the GOM has the same number of striae and fibulae as *P. turgidula* from elsewhere (Almandoz et al., 2008; Hasle and Syvertsen, 1997). Furthermore, the valvocopula and the second band of GOM isolates displayed striations, whereas Lundholm (2000 in Lundholm et al., 2003) reported that the band striae of *P. turgiduloides* lack any kind of ornamentation. Definitive identification of *P. turgidula* isolates from the GOM was further substantiated by sequencing efforts, since both the LSU and ITS2 sequences generated were identical to those obtained for *P. turgidula* isolates from distinct regions, rather than to sequences from *P. turgiduloides*; sequence comparison between both species highlighted several polymorphic sites and species were clearly differentiated in phylogenetic comparisons using both markers. In both the LSU (Fig. 2) and ITS2 (Fig. 3) phylogenies, GOM *P. turgidula* clustered with *P. turgidula* sequences from GenBank, each with 100% bootstrap support for all but one analysis (LSU; MP).

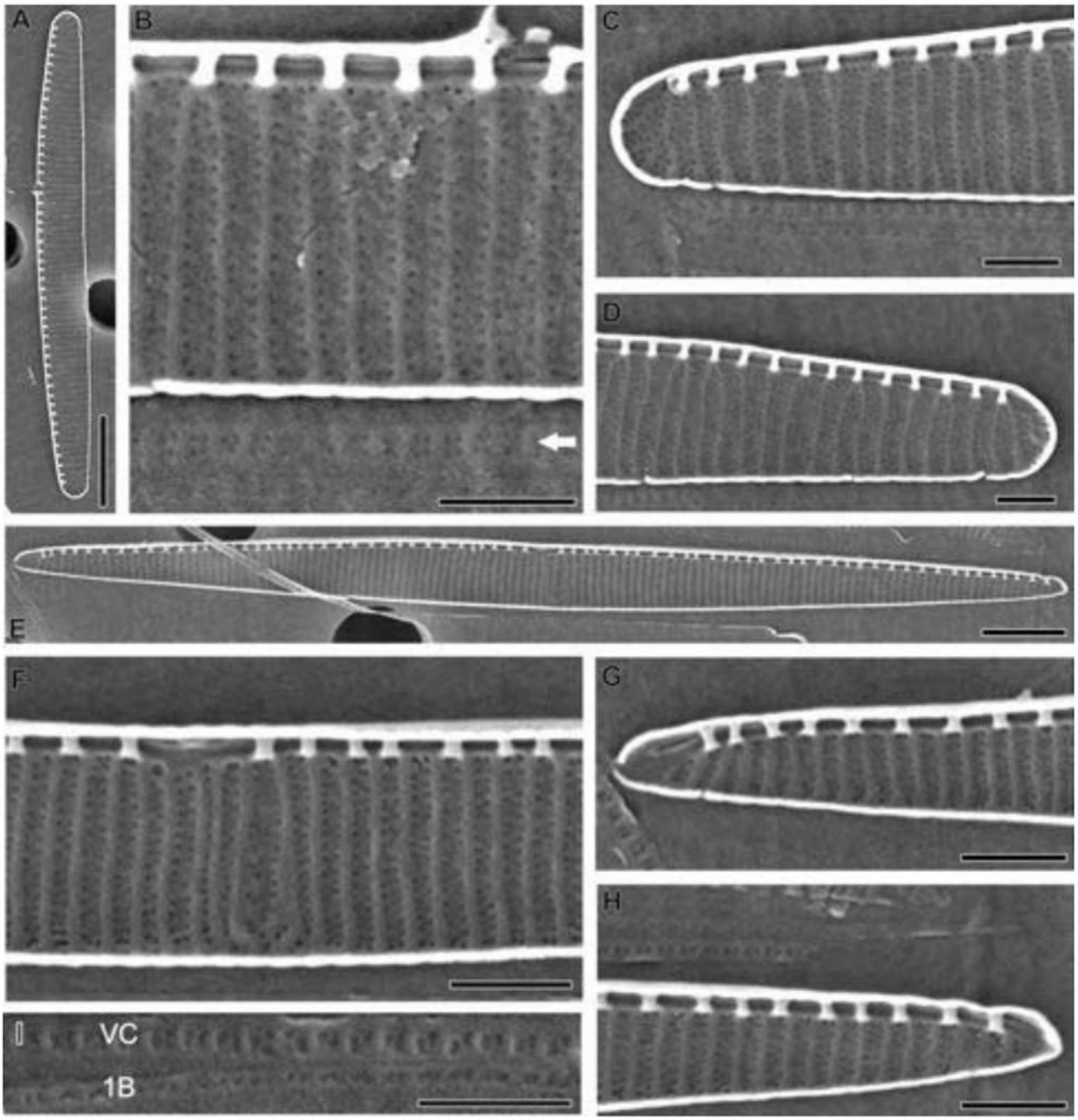

Figure A1.

(A - D). *Pseudo-nitzschia americana*; internal valve views; SEM. (A) General view of valve; (B) center of valve, also showing valvocopula (arrow); (C) and (D) valve apices. **(E - I)** *Pseudo-nitzschia delicatissima*; internal valve views; SEM. (E) Valve in internal view; (F) middle of valve with larger interspace between the central fibulae; (G) and (H) valve apices; (I) detail of valvocopula (VC) and first band (B1). Scale bars: A = 5 μm; B = 1 μm; C-D = 1 μm; E = 5 μm; F-I = 1 μm.

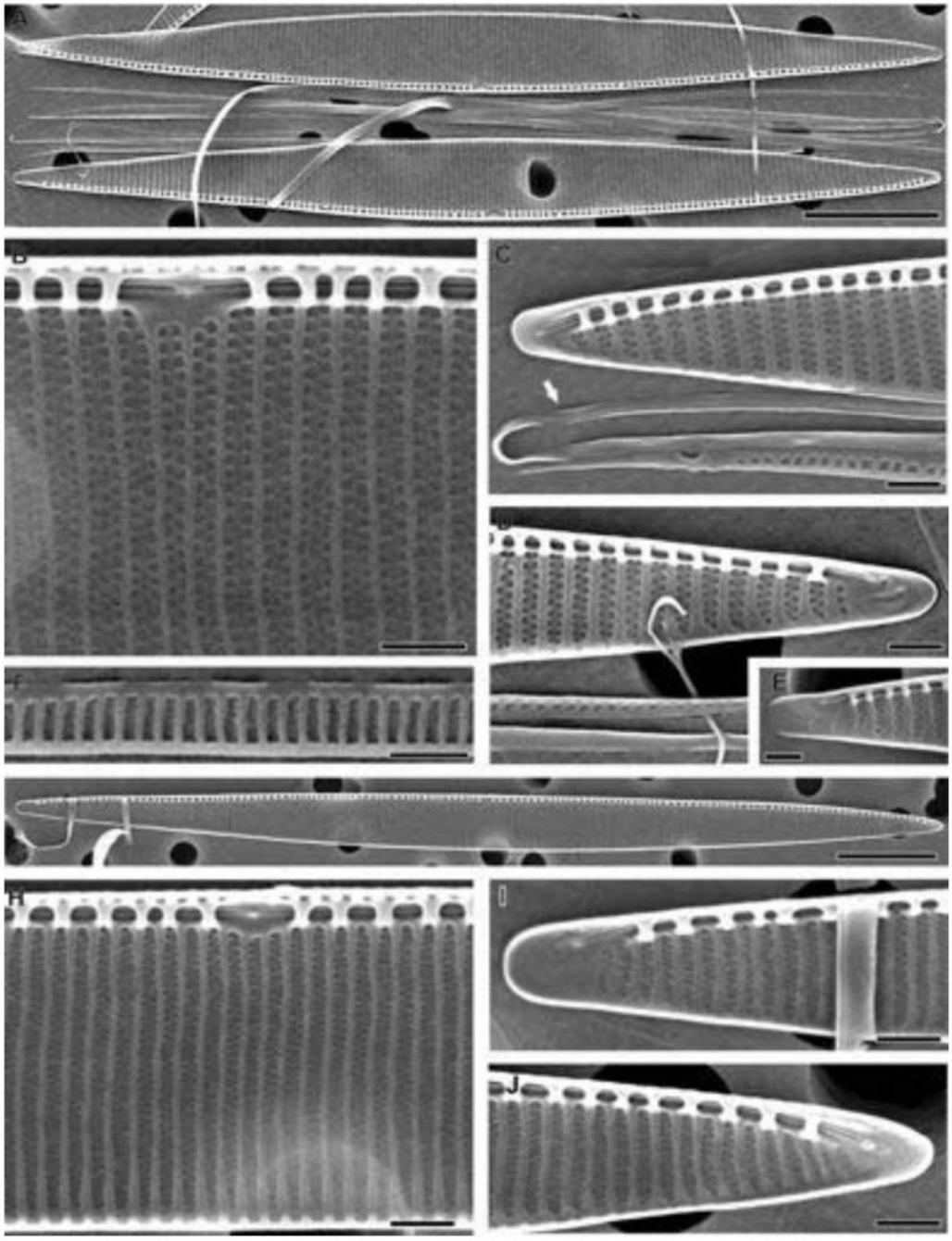

Figure A2.

(A - F). *Pseudo-nitzschia fraudulenta*; internal valve views, SEM. (A) Dismounted frustule, evidencing the two valves and bands of cingulum; (B) center of valve; (C) and (D) valve apices. Note a band lacking poroids in C (arrow); (E) different morphology of apex; (F) detail of valvocopula. **(G - J)** *Pseudo-nitzschia heimii*; internal valve views, SEM. (G) general view of valve; (H) center of valve with a central nodule and larger interspace; (I) and (J) valve apices illustrating their heteropolarity. Scale bars: A = 10 μm; B-F = 1 μm; G = 10 μm; H-J = 1 μm.

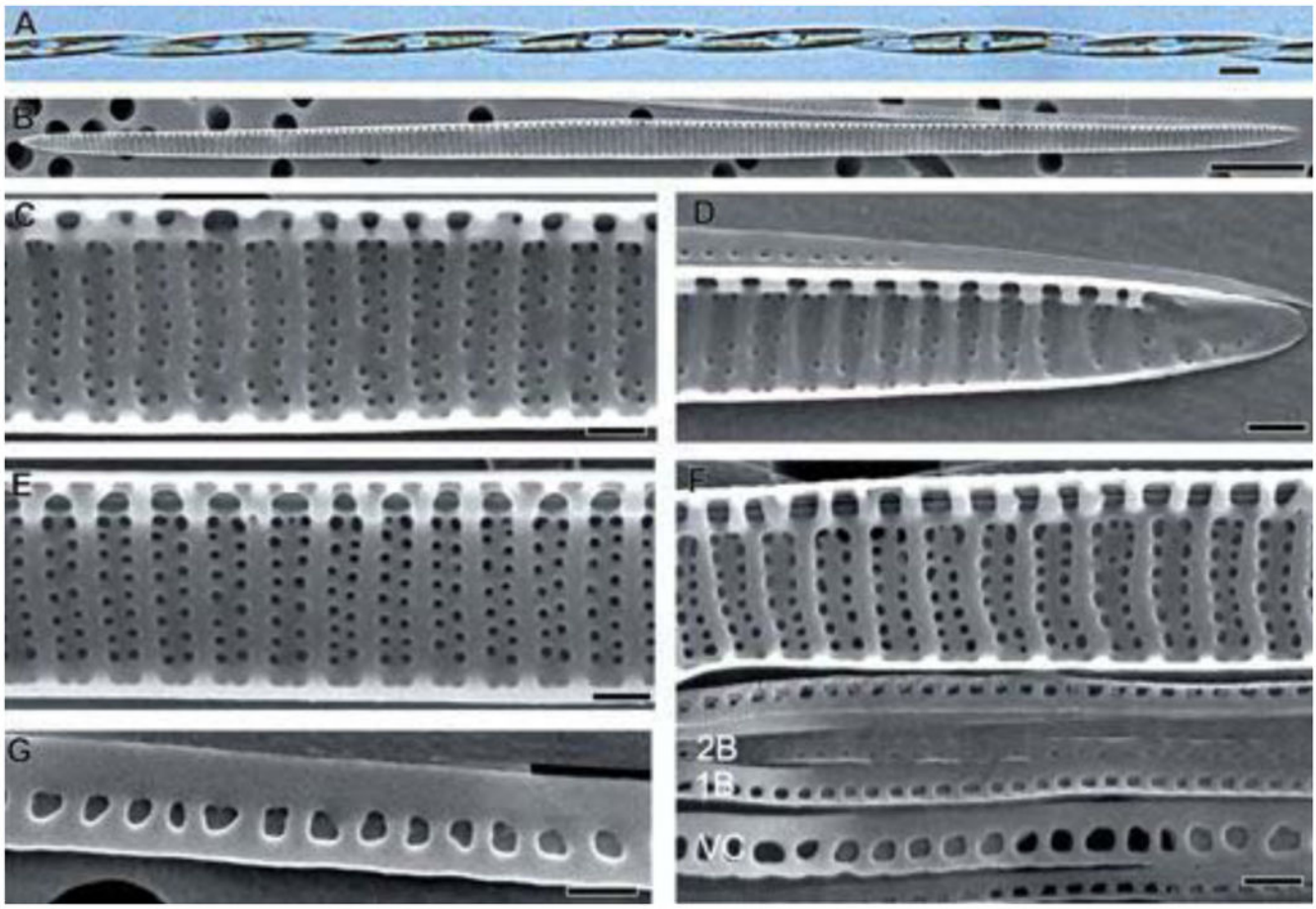

Figure A3.

(A - G). *Pseudo-nitzschia pungens* (A) Living cells in chains, LM. (B - G) internal valve views; SEM. (B) General view of valve; (C) and (E) valve centers, illustrating rows of poroids arranged in different patterns; (D) apex of valve with the ending of valvocopula; (F) center of valve and cingulum. Note the large valvocopula (VC), first band (1B) and second band (2B); (G) detail of a large valvocopula. Scale bars: A-B = 10 μm; C-G = 1 μm.

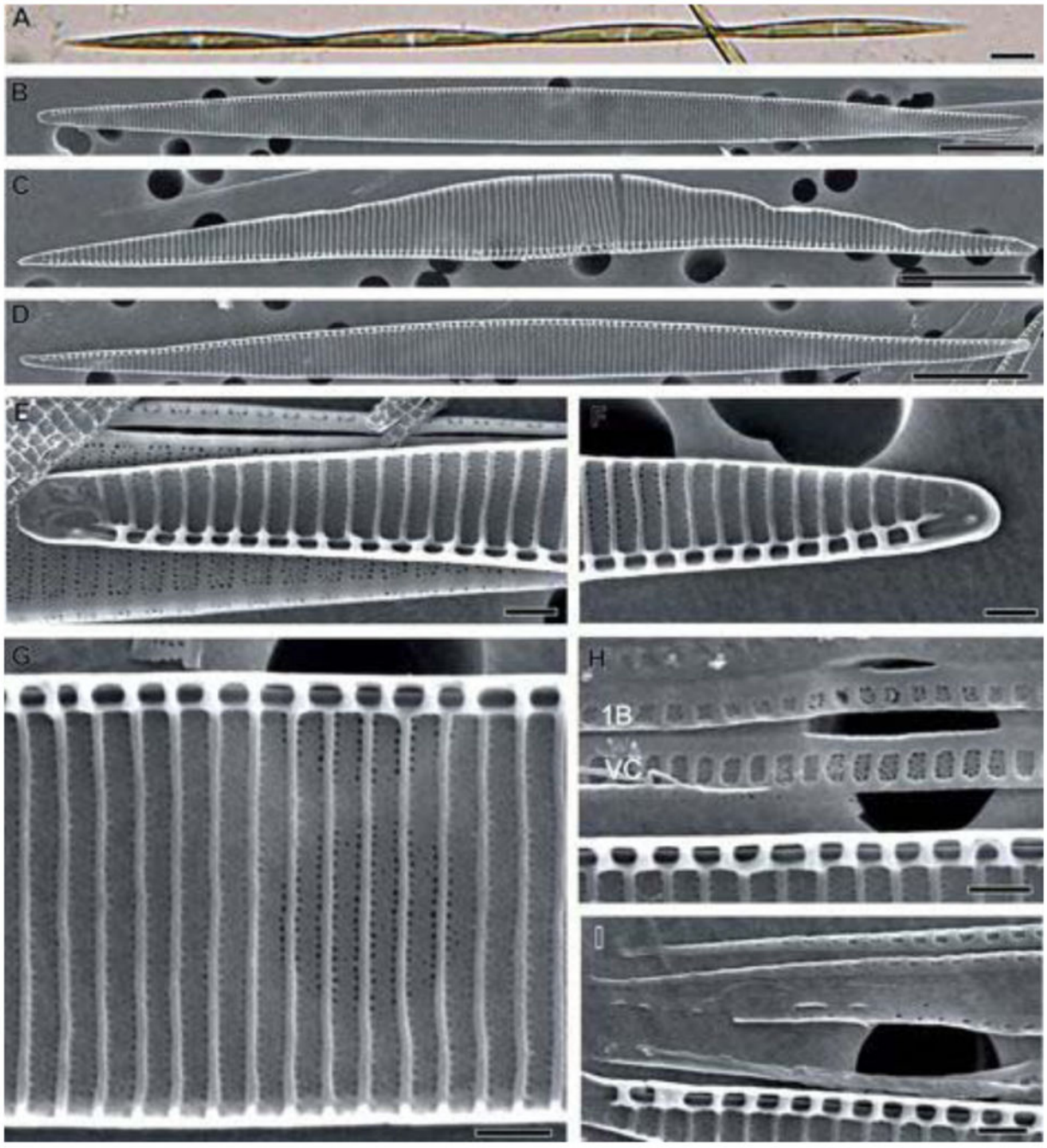

Figure A4.

(A - I). *Pseudo-nitzschia seriata*. (A) Living cells; LM; (B - I) internal views of valve; SEM. (B - D) General views of valves illustrating different valve shapes; (E) and (F) valve apices with the last interstria branched, particularly in E; (G) valve center with fibulae regularly spaced; (H) detail of valvocopula (VC) and first band (B1); (I) Extremities of bands at the valve apex. Scale bars: A = 20 μm; B = 10 μm; C = 8 μm; D = 10 μm; E-I = 1 μm.

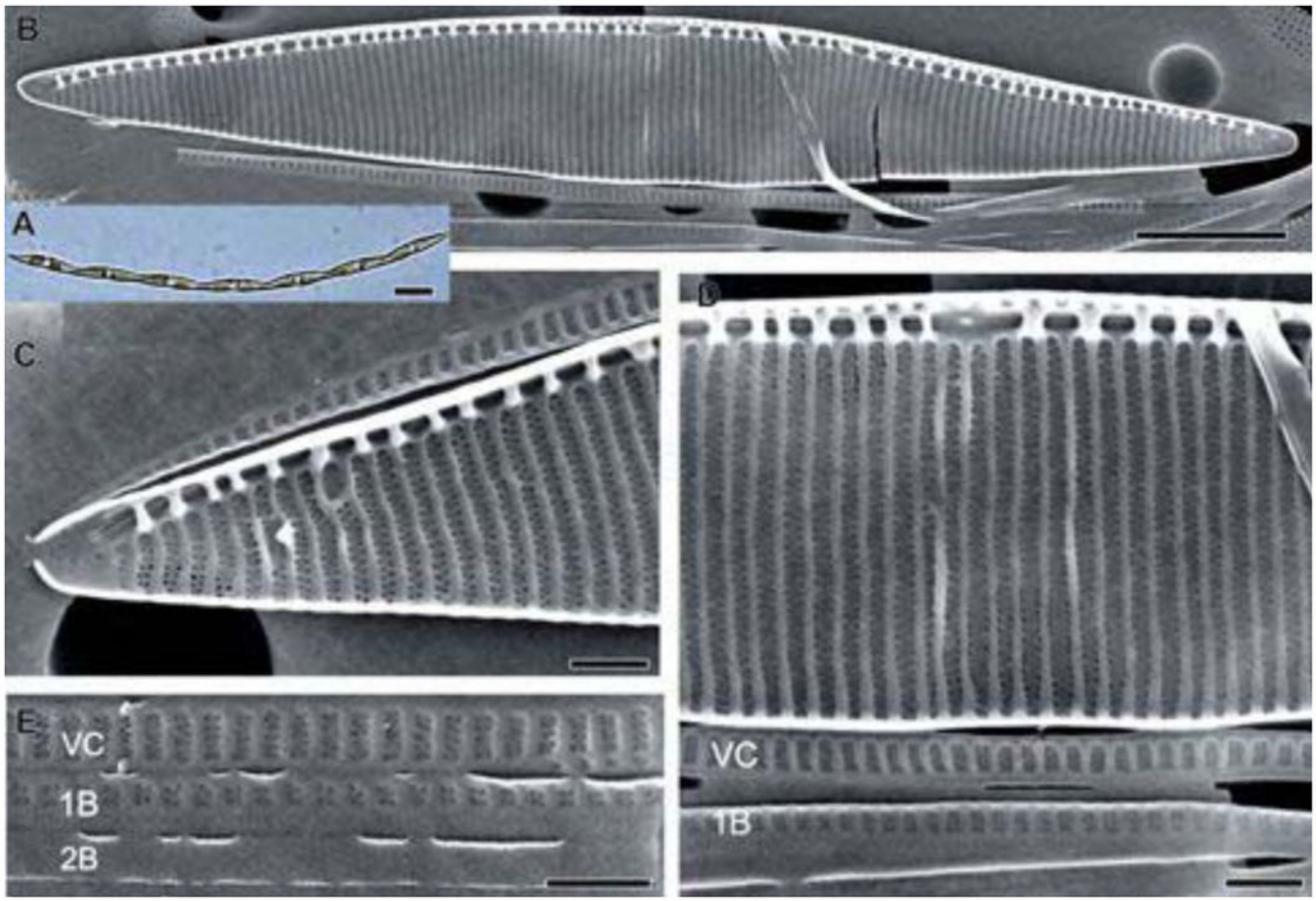

Figure A5.

(A - E). *Pseudo-nitzschia subpacifica*. (A) Living cells in chains; LM; (B - E) internal views of valves; SEM. (B) general view of asymmetric valve; (C) apex of valve, and associated valvocopula; (D) valve center with valvocopula (VC) and first band (1B); (E) detail of cingulum with valvocopula (VC), first band (1B) and second band (2B). Scale bars: A = 20 μm; B = 5 μm; C-E = 1 μm.

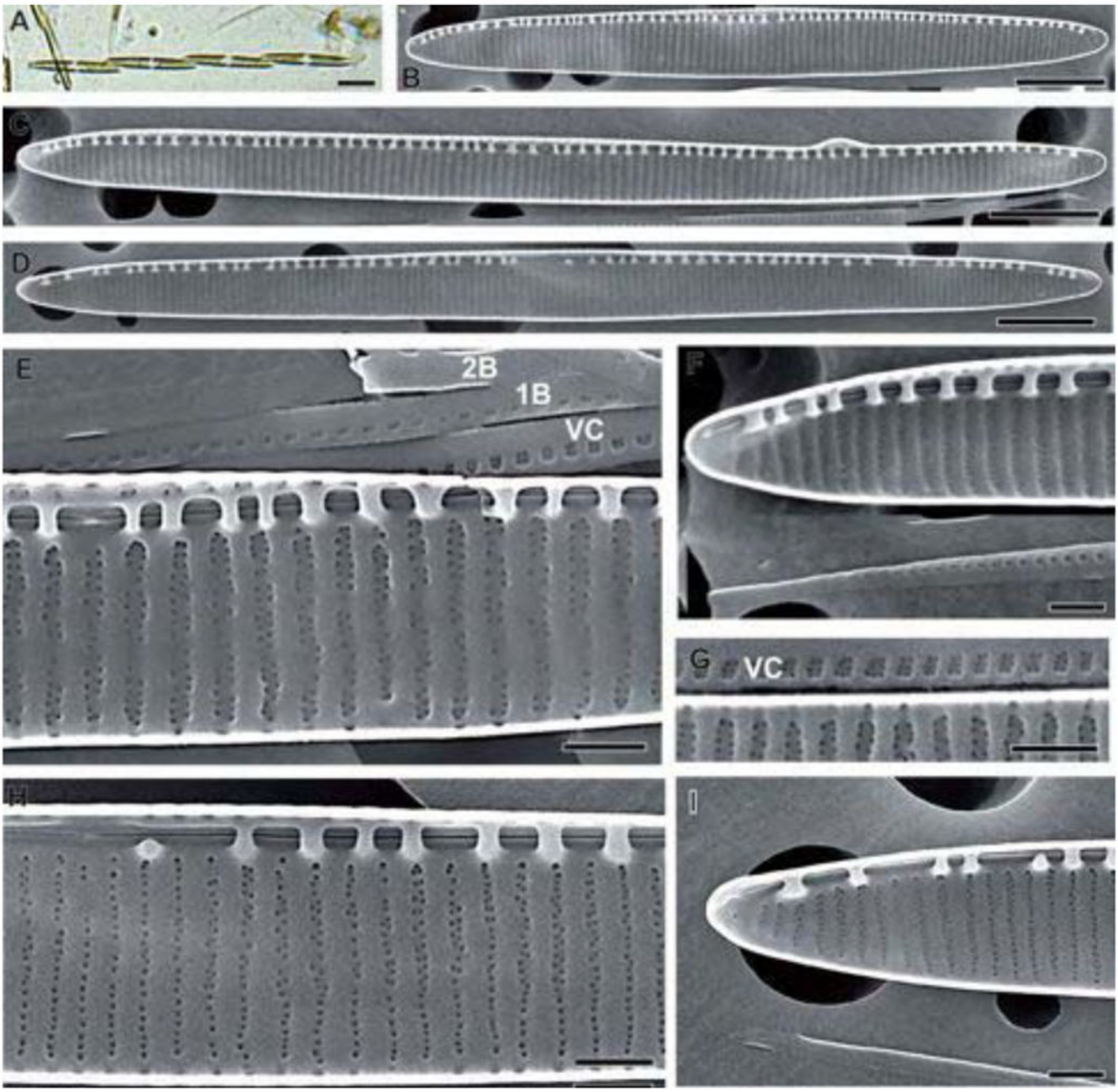

Figure A6.

(A - I). *Pseudo-nitzschia turgidula*. (A) Living cells in chains, LM; (B - I) internal views of valves; SEM. (B), (C) and (D) different shapes of valves, from linear (C) to lanceolate (B and D); (E) center of valve with a central nodule and predominantly two rows of poroids per stria. Note valvocopula (VC), and first (1B) and second (2B) bands; (F) apex of valve and associated ending of valvocopula; (G) valvocopula (VC) at the center of valve; (H) valve center with both one and two rows of poroids per stria; (H) valve apex. Scale bars: A = 20 μm; B-D = 5 μm; E-I = 1 μm.

References

Almandoz GO, Ferreyra GA, Schloss IR, Dogliotti AI, Rupolo V, Paparazzo FE, Esteves JL, Ferrario ME. Distribution and ecology of *Pseudo-nitzschia* species (Bacillariophyceae) in surface waters of the Weddell Sea (Antarctica). Polar Biol. 2008; 31:429–442.

Amato A, Kooistra WHCF, Levialdi Ghiron JH, Mann DG, Pröschold T, Montresor M. Reproductive isolation among sympatric cryptic species in marine diatoms. Protist. 2007; 158:193–207. [PubMed: 17145201]

Amato A, Ludeking A, Kooistra W. Intracellular domoic acid production in *Pseudo-nitzschia multistriata* isolated from the Gulf of Naples (Tyrrhenian Sea, Italy). Toxicon. 2010; 55:157–161. [PubMed: 19615395]

Amato A, Montresor M. Morphology, phylogeny, and sexual cycle of *Pseudo-nitzschia mannii* sp. nov. (Bacillariophyceae): a pseudo-cryptic species within the *P. pseudodelicatissima* complex. Phycologia. 2008; 47:487–497.

Anderson, PS.; Bean, L.; Gladu, S.; Hurst, J.; McGowan, JD.; Standoff, E. The use of citizen-based environmental monitoring programs for making real-time observations about potentially toxigenic phytoplankton. In: Hall, S.; Etheridge, S.; Anderson, D.; Kleindinst, J.; Zhu, M.; Zo, Y., editors. Harmful Algae Management and Mitigation. Asia-Pacific Economic Cooperation (Singapore); Singapore: 2004. p. 131-135.APEC Puplication #204-MR-04.2

Barra L, Ruggiero M, Sarno D, Montresor M, Kooistra WCF. Strengths and weaknesses of microarray approaches to detect *Pseudo-nitzschia* species in the field. Environ Sci Pollut Res. 2012:1–14.

Bates SS. Amnesic shellfish poisoning: domoic acid production by *Pseudo-nitzschia* diatoms. Aqua Info Aquacu. 2004; 16:4. In: http://www.gov.pe.ca/photos/original/af_domoic_acid.pdf.

Bates SS, De Freitas ASW, Milley JE, Pocklington R, Quilliam MA, Smith JC, Worms J. Controls on domoic acid production by the diatom *Nitzschia pungens* f. *multiseries* in culture: nutrients and irradiance. Can J Fish Aquat Sci. 1991; 48:1136–1144.

Bean LL, McGowan JD, Hurst JW Jr. Annual variations of paralytic shellfish poisoning in Maine, USA 1997–2001. Deep Sea Res Part II Top Stud Oceanogr. 2005; 52:2834–2842.

Bigelow HB. Plankton of the offshore waters of the Gulf of Maine. Bull Bureau Fisheries. 1926; 40:1–509.

Bogan YM, Kennedy D, Harkin AL, Gillespie J, Hess P, Slater JW. Comparison of domoic acid concentration in king scallops, *Pecten maximus* from seabed and suspended culture systems. J Shell Res. 2006; 25:129–135.

Cho E, Park J, Oh B, Cho Y. The application of species-specific DNA-based probes and fluorescent tagged lectins for differentiation of several *Pseudo-nitzschia* species (Bacillariophyceae) in Chinhae Bay, Korea. Sci Mar. 2001; 65:207–214.

Coleman AW. ITS2 is a double-edged tool for eukaryote evolutionary comparisons. Trends Genet. 2003; 19:370–375. [PubMed: 12850441]

Couture JY, Levasseur M, Bonneau E, Desjardins C, Sauvé G, Bates SS, Léger C, Gagnon J, Michaud S. Spatial and temporal variation of domoic acid in molluscs and of *Pseudo-nitzschia* spp. blooms in the St. Lawrence from 1998 to 2000. Can Tech Rep Fish Aquat Sci. 2001; 2375:vii, 24.

Darty K, Denise A, Ponty Y. VARNA: Interactive drawing and editing of the RNA secondary structure. Bioinformatics. 2009; 25:1974. [PubMed: 19398448]

Day, G.; Anderson, DM.; Van Dolah, FM.; Taylor, R. Preliminary Investigation of Marine Biotoxins on the Northwest Atlantic Continental Shelf. National Marine Fisheries, NOAA; 2007.

DeGrasse S, Rivera V, Roach J, White K, Callahan J, Couture D, Simon K, Peredy T, Poli M. Paralytic shellfish toxins in clinical matrices: extension of AOAC official method 2005.06 to human urine and serum and application to a 2007 case study in Maine. Deep Sea Res Part II Top Stud Oceanogr. submitted.

Douglas DJ, Kenchington ER, Bird CJ, Pocklington R, Bradford B, Silvert W. Accumulation of domoic acid by the sea scallop (*Placopecten magellanicus*) fed cultured cells of toxic *Pseudo-nitzschia multiseries*. Can J Fish Aquat Sci. 1997; 54:907–913.

Edgar RC. MUSCLE: multiple sequence alignment with high accuracy and high throughput. Nucleic Acids Res. 2004; 32:1792–1797. [PubMed: 15034147]

Evans KM, Bates SS, Medlin LK, Hayes PK. Microsatellite marker development and genetic variation in the toxic marine diatom *Pseudo-nitzschia multiseries* (Bacillariophyceae). J Phycol. 2004; 40:911–920.

FAO. Marine biotoxins. FAO (Food and Agriculture Organization of the United Nations); Rome: 2004. Food and Nutrition Paper 80

Fehling J, Davidson K, Bates SS. Growth dynamics of non-toxic *Pseudo-nitzschia delicatissima* and toxic *P. seriata* (Bacillariophyceae) under simulated spring and summer photoperiods. Harmful Algae. 2005; 4:763–769.

Fehling J, Davidson K, Bolch CJ, Bates SS. Growth and domoic acid production by *Pseudo-nitzschia seriata* (Bacillariophyceae) under phosphate and silicate limitation. Journal of Phycology. 2004; 40:674–683.

Fernandes LF, Brandini FP. The potentially toxic diatom *Pseudo-nitzschia* H. Peragallo in the Paraná and Santa Catarina States, Southern Brazil. Iheringia. Série Botânica. 2010; 65:47–62.

Ferrario, M.; Licea, S.; Balestrini, CF.; Ferreyra, G. Species of *Pseudo-nitzschia* in the Drake Passage (54°–61°S to 46°–64°W). In: Steidinger, KA.; Landsberg, JH.; Tomas, CR.; Vargo, GA., editors. Harmful Algae 2002. Florida Fish and Wildlife Conservation Commission, Florida Institute of Oceanography, and Intergovernmental Oceanographic Commission of UNESCO; St. Petersberg, FL, USA: 2004. p. 434-436.

Fish CJ. Seasonal distribution of the plankton of the Woods Hole region. Bull Bureau Fisheries. 1925; 41:91–179.

Fryxell, G.; Hasle, GA. Taxonomy of harmful diatoms. In: Hallegraeff, GM.; Anderson, DM.; Cembella, AD., editors. Manual on Harmful Marine Microalgae. UNESCO; Paris: 2003. p. 465-509.

Gettings RM, Townsend DW, Thomas MA, Karp-Boss L. Dynamics of late spring and summer phytoplankton communities on Georges Bank, with emphasis on diatoms, *Alexandrium* spp., and other dinoflagellates. Deep Sea Res Part II Top Stud Oceanogr. submitted.

Gilgan, M.; Burns, B.; Landry, G. Distribution and magnitude of domoic acid contamination of shellfish in Atlantic Canada during 1988. In: Granéli, E.; Sundström, B.; Edler, L.; Anderson, DM., editors. Toxic Marine Phytoplankton. Elsevier; New York: 1990. p. 469-474.

Goldstein T, Mazet JAK, Zabka TS, Langlois G, Colegrove KM, Silver M, Bargu S, Van Dolah F, Leighfield T, Conrad PA. Novel symptomatology and changing epidemiology of domoic acid toxicosis in California sea lions (*Zalophus californianus*): an increasing risk to marine mammal health. Proc R Soc B. 2008; 275:267–276.

Gran H. Studies on the Biology and Chemistry of the Gulf of Maine. II. Distribution of phytoplankton in August, 1932. Biol Bull. 1933; 64:159–182.

Gran HH, Braarud T. A quantitative study of the phytoplankton in the Bay of Fundy and the Gulf of Maine (including observations on hydrography, chemistry and turbidity). J Biol Board Can. 1935; 1:279–467.

Hannah CG, Naimie CE, Loder JW, Werner FE. Upper-ocean transport mechanisms from the Gulf of Maine to Georges Bank, with implications for Calanus supply. Cont Shelf Res. 1997; 17:1887–1911.

Hannah CG, Shore JA, Loder JW, Naimie CE. Seasonal circulation on the western and central Scotian Shelf. J Phys Oceanogr. 2001; 31:591–615.

Hansen LR, Kotaki Y, Moestrup Ø, Lundholm N. Toxin production and temperature-induced morphological variation of the diatom *Pseudo-nitzschia seriata* from the Arctic. Harmful Algae. 2011; 10:689–696.

Hargraves P, Maranda L. Potentially toxic or harmful microalgae from the Northeast coast. Northeastern Naturalist. 2002; 9:81–120.

Hasle G, Lange C, Syvertsen E. A review of *Pseudo-nitzschia*, with special reference to the Skagerrak, North Atlantic, and adjacent waters. Helgol Mar Res. 1996; 50:131–175.

Hasle GR. *Nitzschia* and *Fragilariopsis* species studied in the light and electron microscopes II. The group *Pseudonitzschia*. Skr Norske Vidensk-Akad I Mat-Nat Kl Ny Series. 1965; 18:1–45.

Hasle GR. *Pseudo-nitzschia pungens* and *P. multiseries* (Bacillariophyceae): nomenclatural history, morphology, and distribution. J Phycol. 1995; 31:428–435.

Hasle, GR.; Fryxell, GA. Taxonomy of diatoms. In: Hallegraeff, GM.; Anderson, DM.; Cembella, AD., editors. Manual on harmful marine microalgae. UNESCO; Paris, France: 1995. p. 1-22.

Hasle GR, Lundholm N. *Pseudo-nitzschia seriata* f. *obtusa* (Bacillariophyceae) raised in rank based on morphological, phylogenetic and distributional data. Phycologia. 2005; 44:608–619.

Hasle, GR.; Medlin, LK. Family *Bacillariaceae*: the genus *Nitzschia* section Pseudonitzschia. In: Medlin, LK.; Priddle, J., editors. Polar Marine Diatoms. British Antarctic Survey Natural Environment Research Council; Cambridge: 1990. p. 169-176.

Hasle, GR.; Syvertsen, EE. Marine diatoms. In: Tomas, CR., editor. Identifying marine phytoplankton. Academic Press; San Diego: 1997. p. 5-385.

Haya K, Wildish DJ, Martin JL, Burridge LE, Waiwood BA. Domoic acid in shellfish and plankton from the Bay of Fundy, New Brunswick. Canada J Shell Res. 1991; 10:113–118.

Holtermann KE, Bates SS, Trainer VL, Odell A, Armbrust EV. Mass sexual reproduction in the toxigenic diatoms *Pseudo-nitzschia australis* and *P pungens* (Bacillariophyceae) on the Washington coast, USA. J Phycol. 2010; 46:41–52.

Hubbard KA, Rocap G, Armbrust EV. Inter- and intraspecific community structure within the diatom genus *Pseudo-nitzschia* (Bacillariophyceae). J Phycol. 2008; 44:637–649.

James KJ, Gillman M, Amandi MF, Lopez-Rivera A, Puente PF, Lehane M, Mitrovic S, Furey A. Amnesic shellfish poisoning toxins in bivalve molluscs in Ireland. Toxicon. 2005; 46:852–858. [PubMed: 16289180]

Kaczmarska I, LeGresley MM, Martin JL, Ehrman J. Diversity of the diatom genus *Pseudo-nitzschia* Peragallo in the Quoddy Region of the Bay of Fundy, Canada. Harmful Algae. 2005; 4:1–19.

Kaczmarska I, Martin JL, Ehrman JM, LeGresley MM. *Pseudo-nitzschia* species population dynamics in the Quoddy Region, Bay of Fundy. Harmful Algae. 2007; 6:861–874.

Kaczmarska I, Reid C, Martin JL, Moniz MBJ. Morphological, biological, and molecular characteristics of the diatom *Pseudo-nitzschia delicatissima* from the Canadian Maritimes. Botany. 2008; 86:763–772.

Kenney R, Winn H. Cetacean high-use habitats of the northeast United States continental shelf. Fish Bull(United States). 1986; 84

Kleindinst JL, Anderson DM, McGillicuddy DJ J, S RP, Fisher KM, Couture DA, Hickey JM, Nash C. Categorizing the severity of paralytic shellfish poisoning outbreaks in the Gulf of Maine for forecasting and management. Deep Sea Res Part II Top Stud Oceanogr. submitted.

Leandro LF, Rolland RM, Roth PB, Lundholm N, Wang Z, Doucette GJ. Exposure of the North Atlantic right whale *Eubalaena glacialis* to the marine algal biotoxin, domoic acid. Mar Ecol Prog Ser. 2010; 398:287–303.

Lefebvre KA, Frame ER, Gulland F, Hansen JD, Kendrick PS, Beyer RP, Bammler TK, Farin FM, Hiolski EM, Smith DR. A novel antibody-based biomarker for chronic algal toxin exposure and sub-acute neurotoxicity. PloS One. 2012; 7:e36213. [PubMed: 22567140]

Lefebvre KA, Robertson A. Domoic acid and human exposure risks: a review. Toxicon. 2010; 56:218–230. [PubMed: 19505488]

Lelong A, Bucciarelli E, Hégaret H, Soudant P. Iron and copper limitations differently affect growth rates and photosynthetic and physiological parameters of the marine diatom *Pseudo-nitzschia delicatissima*. Limnol Oceanogr. 2013; 58:613–623.

Lelong A, Hégaret H, Soudant P, Bates SS. *Pseudo-nitzschia* (Bacillariophyceae) species, domoic acid and amnesic shellfish poisoning: revisiting previous paradigms. Phycologia. 2012; 51:168–216.

Lewitus AJ, Horner RA, Caron DA, Garcia-Mendoza E, Hickey BM, Hunter M, Huppert DD, Kudela RM, Langlois GW, Largier JL. Harmful algal blooms along the North American west coast region: History, trends, causes, and impacts. Harmful Algae. 2012; 19:133–159.

Li WKW, Andersen RA, Gifford DJ, Incze LS, Martin JL, Pilskaln CH, Rooney-Varga JN, Sieracki ME, Wilson WH, Wolff NH. Planktonic microbes in the Gulf of Maine area. PloS One. 2011; 6:e20981. [PubMed: 21698243]

Lillick LC. Seasonal studies of the phytoplankton off Woods Hole. Massachusetts Biol Bull. 1937; 73:488–503.

Lillick LC. Phytoplankton and planktonic protozoa of the offshore waters of the Gulf of Maine. Part II. Qualitative composition of the planktonic flora. Trans Amer Phil Soc. 1940; 31:193–237.

Lim HC, Leaw CP, Su SNP, Teng ST, Usup G, Mohammad Noor N, Lundholm N, Kotaki Y, Lim PT. Morphology and molecular characterization of *Pseudo-nitzschia* (Bacillariophyceae) From Malaysian Borneo, including the new species *Pseudo-nitzschia circumpora* sp. nov. J Phycol. 2012; 48

Lundholm N, Bates SS, Baugh KA, Bill BD, Connell LB, Léger C, Trainer VL. Cryptic and pseudo cryptic diversity in diatoms—with descriptions of *Pseudo nitzschia hasleana* sp. nov. and *P. fryxelliana* sp. nov. J Phycol. 2012; 48:436–454.

Lundholm N, Clarke A, Ellegaard M. A 100-year record of changing *Pseudo-nitzschia* species in a sill-fjord in Denmark related to nitrogen loading and temperature. Harmful Algae. 2010; 9:449–457.

Lundholm N, Hasle GR, Fryxell GA, Hargraves PE. Morphology, phylogeny and taxonomy of species within the *Pseudo-nitzschia americana* complex (Bacillariophyceae) with descriptions of two new species, *Pseudo-nitzschia brasiliana* and *Pseudo-nitzschia linea*. Phycologia. 2002; 41:480–497.

Lundholm N, Moestrup Ø, Hasle GR, Hoef-Emden K. A study of the *Pseudo-nitzschia pseudodelicatissima/cuspidata* complex (Bacillariophyceae): what is *P. pseudodelicatissima*? J Phycol. 2003; 39:797–813.

Lundholm N, Skov J, Pocklington R, Moestrup Ø. Domoic acid, the toxic amino acid responsible for amnesic shellfish poisoning, now in *Pseudonitzschia seriata* (Bacillariophyceae) in Europe. Phycologia. 1994; 33:475–478.

Mafra LL Jr, Léger C, Bates SS, Quilliam MA. Analysis of trace levels of domoic acid in seawater and plankton by liquid chromatography without derivatization, using UV or mass spectrometry detection. J Chromatogr A. 2009; 1216:6003–6011. [PubMed: 19577240]

Mai JC, Coleman AW. The internal transcribed spacer 2 exhibits a common secondary structure in green algae and flowering plants. J Molec Evol. 1997; 44:258–271. [PubMed: 9060392]

Marchetti A, Lundholm N, Kotaki Y, Hubbard K, Harrison PJ, Armbrust VE. Identification and assessment of domoic acid production in oceanic *Pseudo-nitzschia* (Bacillariophyceae) from iron-limited waters in the northeast subarctic Pacific. J Phycol. 2008; 44:650–661.

Marin B, Klingberg M, Melkonian M. Phylogenetic Relationships among the Cryptophyta: Analyses of Nuclear-Encoded SSU rRNA Sequences Support the Monophyly of Extant Plastid-Containing Lineages. Protist. 1998; 149:265–276. [PubMed: 23194638]

Marshall, HG. Rapports et Proces-verbaux des Reunions. Vol. 183. Conseil International pour l'Exploration de la Mer; 1984. Phytoplankton of the northeastern continental shelf of the United States in relation to abundance, composition, cell volume, seasonal, and regional assemblages; p. 31-50.

Marshall, HG.; Cohn, MS. Phytoplankton community structure in northeastern coastal waters of the United States for November 1978. NOAA Technical memorandum NMFS-F/NEC-9 National Marine Fisheries Service; Woods Hole, MA: 1981. p. 1-43.

Marshall, HG.; Cohn, MS. NOAA Technical memorandum NMFS-F/NEC-8. National Marine Fisheries Service; Woods Hole, MA: 1981. Phytoplankton community structure in northeastern coastal waters of the United States for October 1978; p. 1-49.

Marshall, HG.; Cohn, MS. Seasonal phytoplankton assemblages in northeastern waters of the United States. National Marine Fisheries Service; Woods Hole, MA: 1982. p. 1-31.NOAA Technical memorandum NMFS-F/NEC-15

Marshall HG, Cohn MS. Distribution and composition of phytoplankton in northeastern coastal waters of the United States. Estuar Coast Shelf Sci. 1983; 17:119–131.

Marshall HG, Cohn MS. Phytoplankton composition of the New York Bight and adjacent waters. J Plankton Res. 1987; 9:267–276.

Martin JL, Haya K, Burridge L, Wildish D. *Nitzschia pseudodelicatissima* - a source of domoic acid in the Bay of Fundy, eastern Canada. Mar Ecol Prog Ser. 1990; 6:177–182.

Martin, JL.; Page, FH.; LeGresley, MM.; Richard, DJA. Phytoplankton monitoring as a management tool: Timing of *Alexandrium* and *Pseudo-nitzschia* blooms in the Bay of Fundy, Eastern Canada. In: Hall, S.; Etheridge, S.; Anderson, D.; Kleindinst, J.; M, Z.; Zou, Y., editors. Harmful Algae Management and Mitigation. Asia-Pacific Economic Cooperation (Singapore); 2004. p. 136-140.APEC Puplication #204-MR-04.2

McDonald SM, Sarno D, Zingone A. Identifying *Pseudo-nitzschia* species in natural samples using genus-specific PCR primers and clone libraries. Harmful Algae. 2007; 6:849–860.

McGillicuddy DJ, Anderson DM, Solow AR, Townsend DW. Interannual variability of *Alexandrium fundyense* abundance and shellfish toxicity in the Gulf of Maine. Deep Sea Res Part II Top Stud Oceanogr. 2005; 52:2843–2855.

McGillicuddy DJ Jr, Townsend DW, Keafer BA, Thomas MA, Anderson DM. Georges Bank: a leaky incubator of *Alexandrium fundyense* blooms. Deep Sea Res Part II Top Stud Oceanogr. submitted.

Moschandreou KK, Nikolaidis G. The genus *Pseudo-nitzschia* (Bacillariophyceae) in Greek coastal waters. Botanica Marina. 2010; 53:159–172.

Moschandreou KK, Papaefthimiou D, Katikou P, Kalopesa E, Panou A, Nikolaidis G. Morphology, phylogeny and toxin analysis of *Pseudo-nitzschia pseudodelicatissima* (Bacillariophyceae) isolated from the Thermaikos Gulf, Greece. Phycologia. 2010; 49:260–273.

Orive E, Laza-Martinez A, Seoane S, Alonso A, Andrade R, Miguel I. Diversity of *Pseudo-nitzschia* in the southeastern Bay of Biscay. Diatom Res. 2010; 25:125–145.

Orsini L, Procaccini G, Sarno D, Montresor M. Multiple rDNA ITS-types within the diatom *Pseudo-nitzschia delicatissima* (Bacillariophyceae) and their relative abundances across a spring bloom in the Gulf of Naples. Mar Ecol Prog Ser. 2004; 271:87–98.

Pearson H. Toxic algae suspected in whale death. Nature News. 200310.1038/news030804-l

Perl TM, Bédard L, Kosatsky T, Hockin JC, Todd ECD, Remis RS. An outbreak of toxic encephalopathy caused by eating mussels contaminated with domoic acid. N Engl J Med. 1990; 322:1775–1780. [PubMed: 1971709]

Pettigrew NR, Churchill JH, Janzen CD, Mangum LJ, Signell RP, Thomas AC, Townsend DW, Wallinga JP, Xue H. The kinematic and hydrographic structure of the Gulf of Maine Coastal Current. Deep Sea Res Part II Top Stud Oceanogr. 2005; 52:2369–2391.

Picot C, Nguyen TA, Roudot AC, Parent-Massin D. A preliminary risk assessment of human exposure to phycotoxins in shellfish: a review. Hum Ecol Risk Assess. 2011; 17:328–366.

Pitcher GC, Figueiras FG, Hickey BM, Moita MT. The physical oceanography of upwelling systems and the development of harmful algal blooms. Prog Oceanogr. 2010; 85:5–32. [PubMed: 22053120]

Pocklington R, Milley JE, Bates SS, Bird CJ, De Freitas ASW, Quilliam MA. Trace determination of domoic acid in sea water and phytoplankton by high-performance liquid chromatography of the fluorenylmethoxycarbonyl (FMOC) derivative. Int J Environ Anal Chem. 1990; 38:351–368.

Posada D, Crandall KA. MODEL TEST: testing the model of DNA substitution. Bioinformatics. 1998; 14:817–818. [PubMed: 9918953]

Quijano-Scheggia S, Garcés E, Sampedro N, van Lenning K, Flo E, Andree K, Fortuño JM, Camp J. Identification and characterisation of the dominant *Pseudo-nitzschia* species (Bacillariophyceae) along the NE Spanish coast (Catalonia, NW Mediterranean). Sci Mar. 2008; 72

Scholin C, Buck K, Britschgi T, Cangelosi G, Chavez F. Identification of *Pseudo-nitzschia australis* (Bacillariophyceae) using rRNA-targeted probes in whole cell and sandwich hybridization formats. Phycologia. 1996; 35:190–197.

Scholin CA, Villac MC, Buck KR, Krupp JM, Powers DA, Fryxell GA, Chavez FP. Ribosomal DNA sequences discriminate among toxic and non-toxic *Pseudonitzschia* species. Nat Toxins. 1994; 2:152–165. [PubMed: 7952939]

Skov, J.; Lundholm, N.; Moestrup, Ø.; Larsen, J. Potentially toxic phytoplankton. 4. The diatom genus *Pseudo-nitzschia* (Diatomophyceae/Bacillariophyceae). In: Lindley, JA., editor. ICES Identif Leaflets Plankton. Vol. 185. 1999. p. 1-23.

Smith MW, Maier MA, Suciu D, Peterson TD, Bradstreet T, Nakayama J, Simon HM. High resolution microarray assay for rapid taxonomic assessment of *Pseudo-nitzschia* spp. (Bacillariophyceae) in the field. Harmful Algae. 2012; 19:169–180.

Stewart JE, Marks L, Gilgan M, Pfeiffer E, Zwicker B. Microbial utilization of the neurotoxin domoic acid: blue mussels (*Mytilus edulis*) and soft shell clams (*Mya arenaria*) as sources of the microorganisms. Can J Microbiol. 1998; 44:456–464. [PubMed: 9741971]

Swofford, DL. PAUP: Phylogenetic analysis using parsimony and other methods (software), 4.0 Beta. 10. Sinauer Associates; Sunderland, MA: 2000.

Thomas AC, Townsend DW, Weatherbee R. Satellite-measured phytoplankton variability in the Gulf of Maine. Cont Shelf Res. 2003; 23:971–989.

Thompson JD, Higgins DG, Gibson TJ. CLUSTAL W: improving the sensitivity of progressive multiple sequence alignment through sequence weighting, position-specific gap penalties and weight matrix choice. Nucleic Acids Res. 1994; 22:4673–4680. [PubMed: 7984417]

Townsend DW, Rebuck ND, Thomas MA, Karp-Boss L, Gettings RM. A changing nutrient regime in the Gulf of Maine. Continental Shelf Research. 2010a; 30:820–832.

Townsend DW, Rebuck ND, Thomas MA, Karp-Boss L, Gettings RM. A changing nutrient regime in the Gulf of Maine. Cont Shelf Res. 2010b; 30:820–832.

Trainer VL, Bates SS, Lundholm N, Thessen AE, Adams NG, Cochlan WP, Trick CG. *Pseudo-nitzschia* physiological ecology, phylogeny, toxicity, monitoring and impacts on ecosystem health. Harmful Algae. 2012; 14:271–300.

Trainer, VL.; Hickey, BM.; Bates, SS. Toxic diatoms. In: Walsh, PJ.; Smith, SL.; Fleming, LE.; Solo-Gabriele, H.; Gerwick, WH., editors. Oceans and Human Health: Risks and Remedies from the Sea. Elsevier Science Publishers; New York: 2008. p. 219-238.

Trainer VL, Hickey BM, Lessard EJ, Cochlan WP, Trick CG, Wells ML, MacFadyen A, Moore SK. Variability of *Pseudo-nitzschia* and domoic acid in the Juan de Fuca eddy region and its adjacent shelves. Limnol Oceanogr. 2009a; 54:289–308.

Trainer VL, Wells ML, Cochlan WP, Trick CG, Bill BD, Baugh KA, Beall BF, Herndon J, Lundholm N. An ecological study of a massive bloom of toxigenic Pseudo-nitzschia cuspidata off the Washington State coast. Limnol Oceanogr. 2009b; 54:1461.

Van Egmond, H.; ME, VA.; Speijers, G. Amnesic shellfish poisoning (ASP). In: Van Egmond, H.; ME, VA.; Speijers, G., editors. Marine Biotoxins. Food and Agriculture Organization of the United Nations; Rome, Italy: 2004. p. 97-135.

Villac M, Fryxell G. *Pseudo-nitzschia pungens* var. *cingulata* var. nov.(Bacillariophyceae) based on field and culture observations. Phycologia. 1998; 37:269–274.

Villareal TA, Roelke DL, Fryxell GA. Occurrence of the toxic diatom *Nitzschia pungens* f. *multiseries* in Massachusetts Bay, Massachusetts, USA. Marine Environ Res. 1994; 37:417–423.

Waring G, Josephson E, Maze-Foley K, Rosel P. U.S. Atlantic and Gulf of Mexico Marine Mammal Stock Assessments-2011. NOAA Tech Memo NMFS NE. 2012; 221:319.

Wohlgeschaffen GD, Mann KH, Subba Rao DV, Pocklington R. Dynamics of the phycotoxin domoic acid: accumulation and excretion in two commercially important bivalves. J Appl Phycol. 1992; 4:297–310.

Zuker M. Mfold web server for nucleic acid folding and hybridization prediction. Nucleic Acids Res. 2003; 31:3406–3415. [PubMed: 12824337]

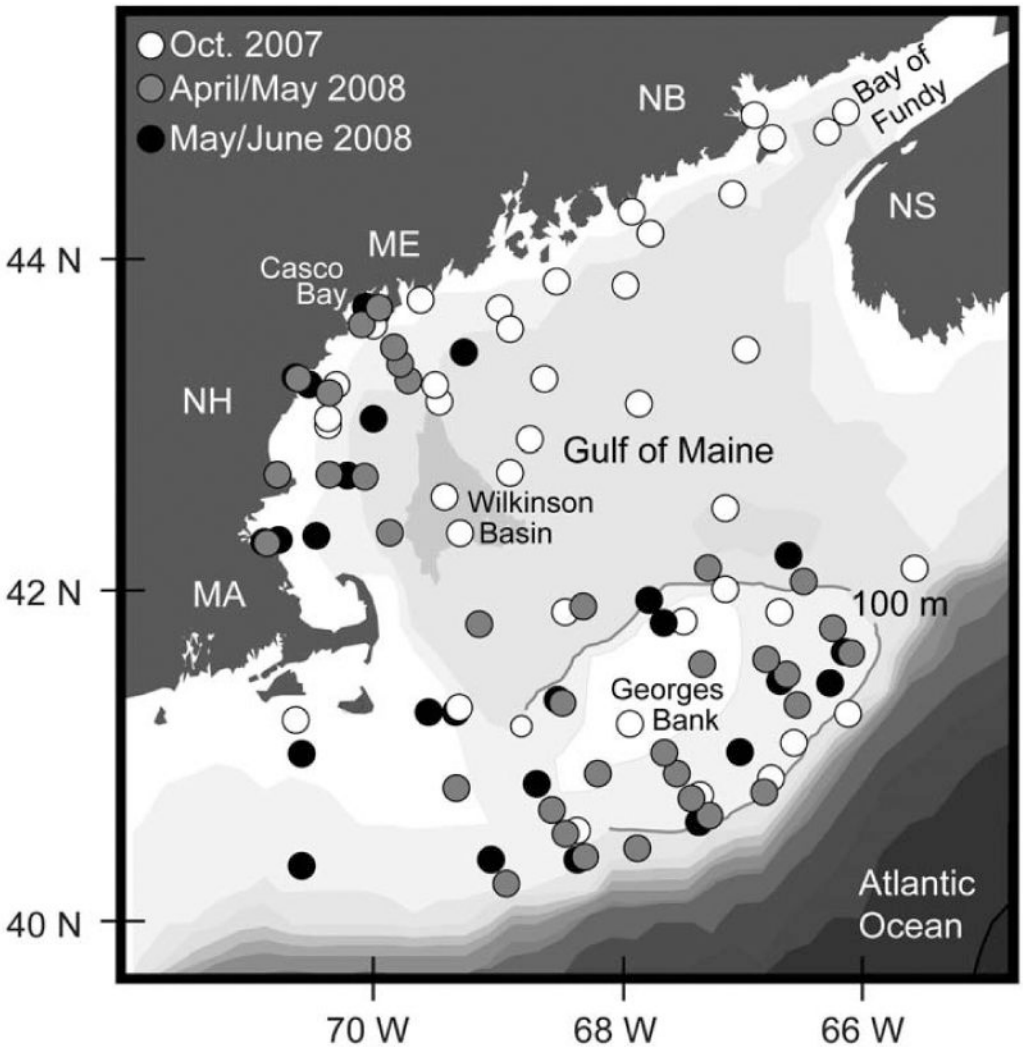

Figure 1.
Map of the GOM showing sample collection locations, 2007-2008.

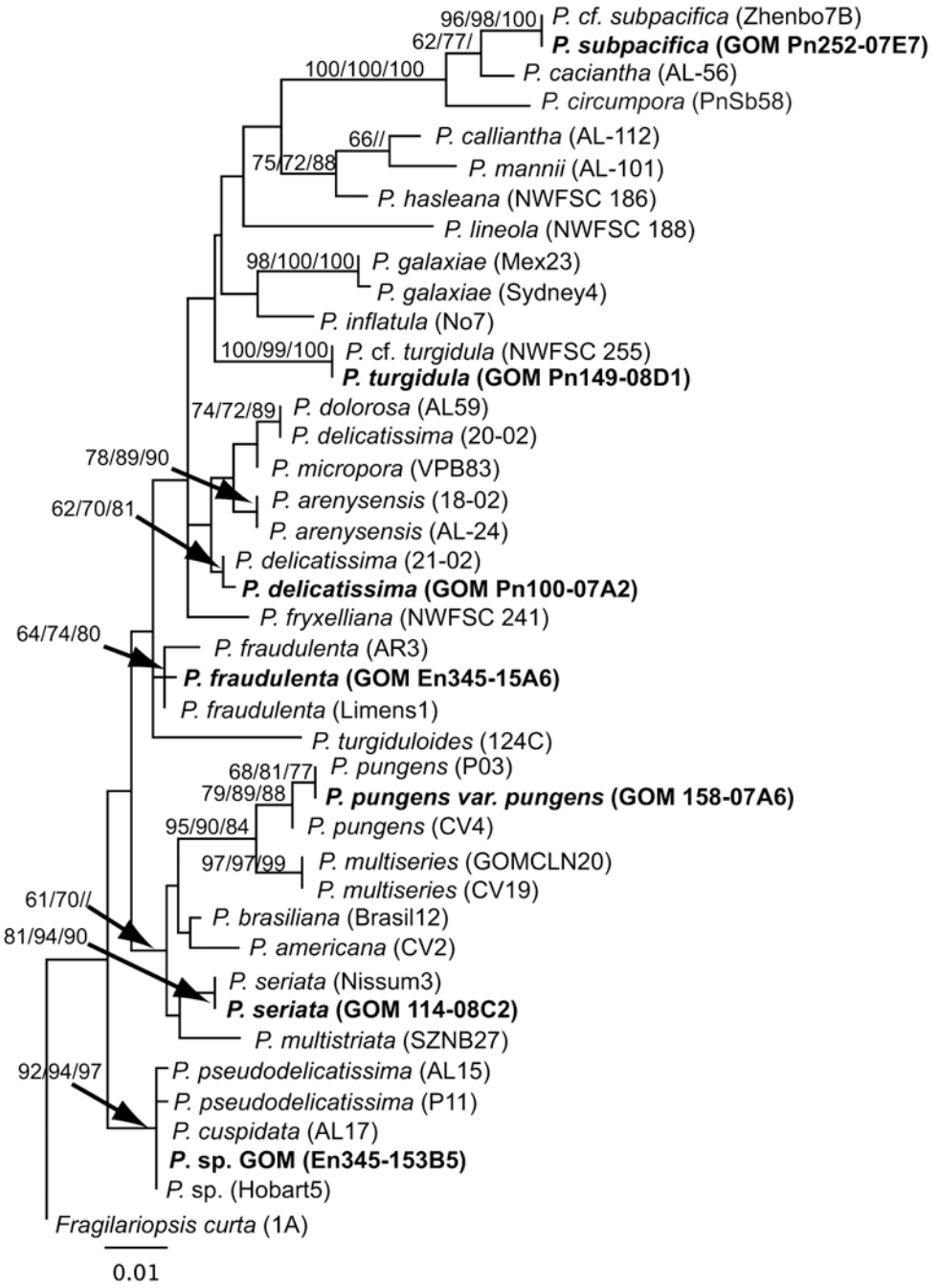

Figure 2.

Maximum likelihood tree inferred from partial LSU sequences of the rRNA gene of *Pseudo-nitzschia* from the GOM. Bootstrap values above 60% based on 100 replicates of ML, MP and NJ analyses are shown adjacent to each node. Isolates identified by the current study are in bold. Strain names and GenBank accession numbers are shown next to each species.

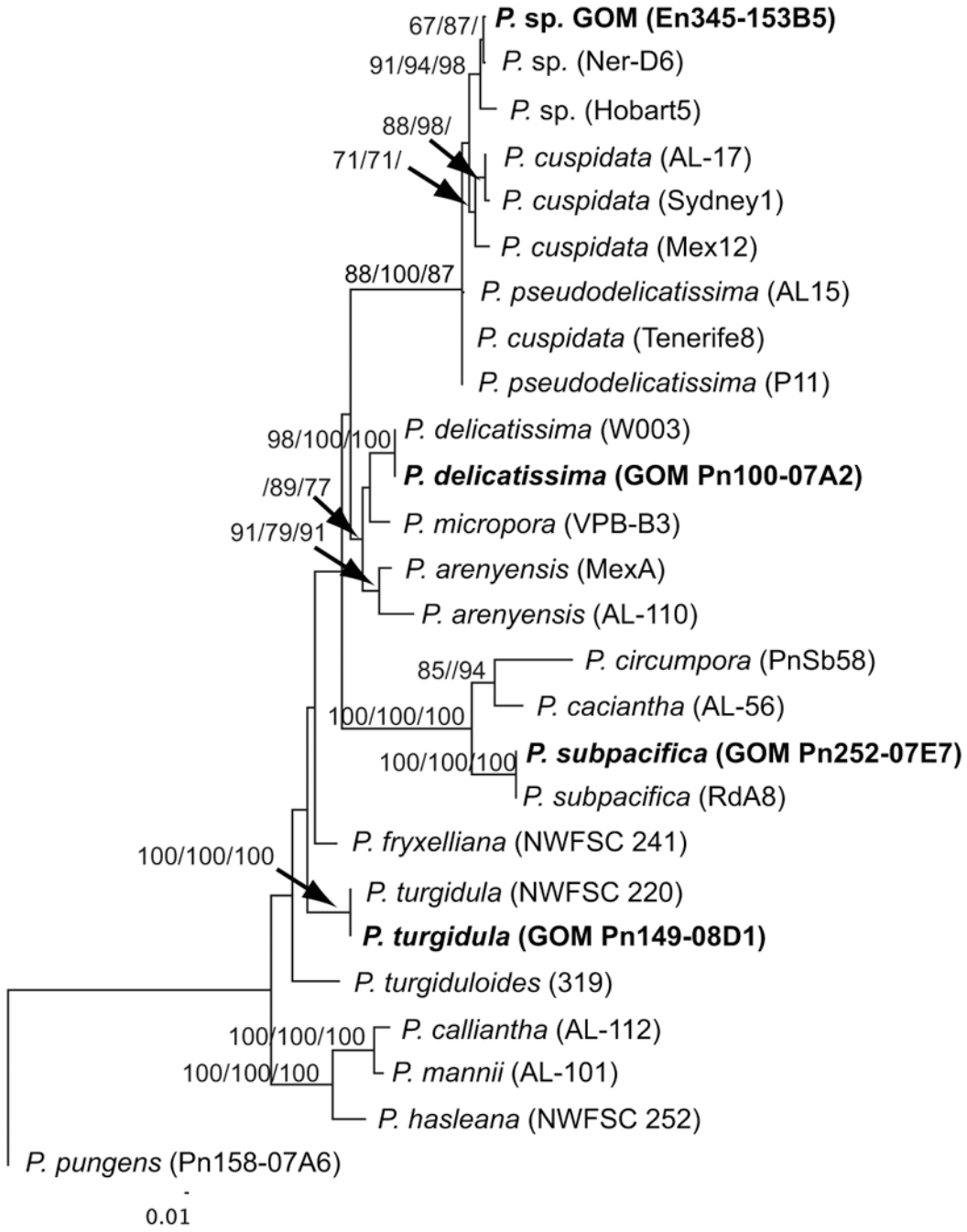

Figure 3.

Maximum likelihood tree inferred from ITS2 sequences of the rRNA gene of *Pseudo-nitzschia pseudodelicatissima, P. delicatissima, P. subpacifica* and *P. turgidula* from the GOM. Bootstrap values above 60% based on 100 replicates of ML, MP and NJ analyses are shown adjacent to each node. Isolates identified by the current study are in bold. Strain names and GenBank accession numbers are shown next to each species.

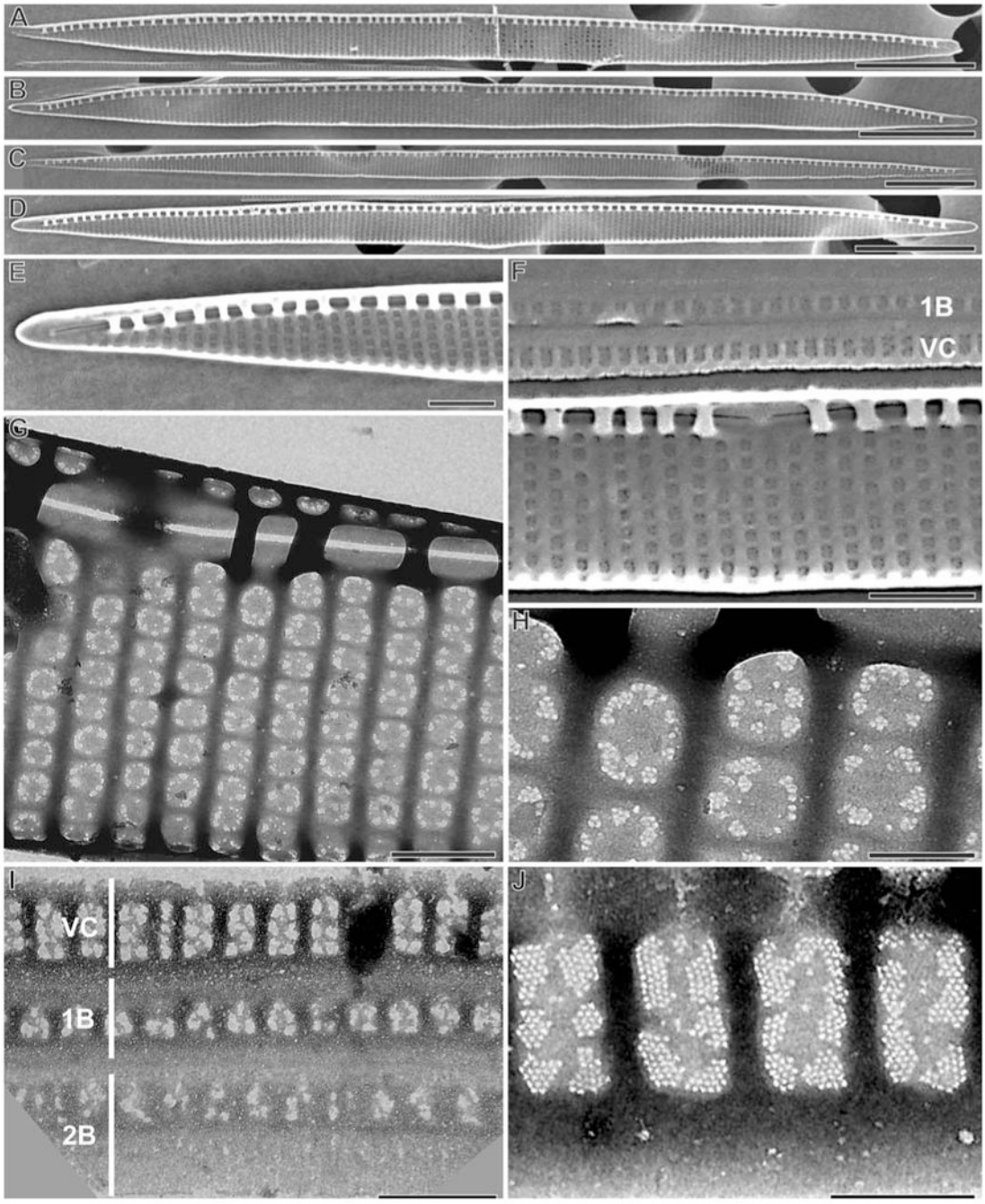

Figure 4.

(A - J). *Pseudo-nitzschia* sp. GOM. (A - F) internal view of valves, SEM. (G -J) TEM. (A - B) General view of strains Pn236-07A2 and Pn202-07A8 respectively, illustrating differences in shape, especially at the apices; (C) slender valve with pointed apices of strain Pn236-07A6; (D) strain En435-153-B5. (E – F): strain Pn236-07A2. (E) valve apex; (F) center of valve with central nodule. Cingulum with valvocopula (VC) and first band (1B) are also showed; (G) Detail of central nodule and large central interspace; (H) Poroids possessing numerous and irregular sectors; (I) Cingular bands. Valvocopula (VC), first (1B)

and second (2B) bands; (J) Detail of valvocopula showing four striae, each one 2 poroid wide and 2-3 poroid high. Note irregular hymenated poroids. Scale bars: A – D = 5 μm; E – F = 1 μm; G = 0.5 μm; H = 0.2 μm; I = 0.5 μm; J = 0.2 μm

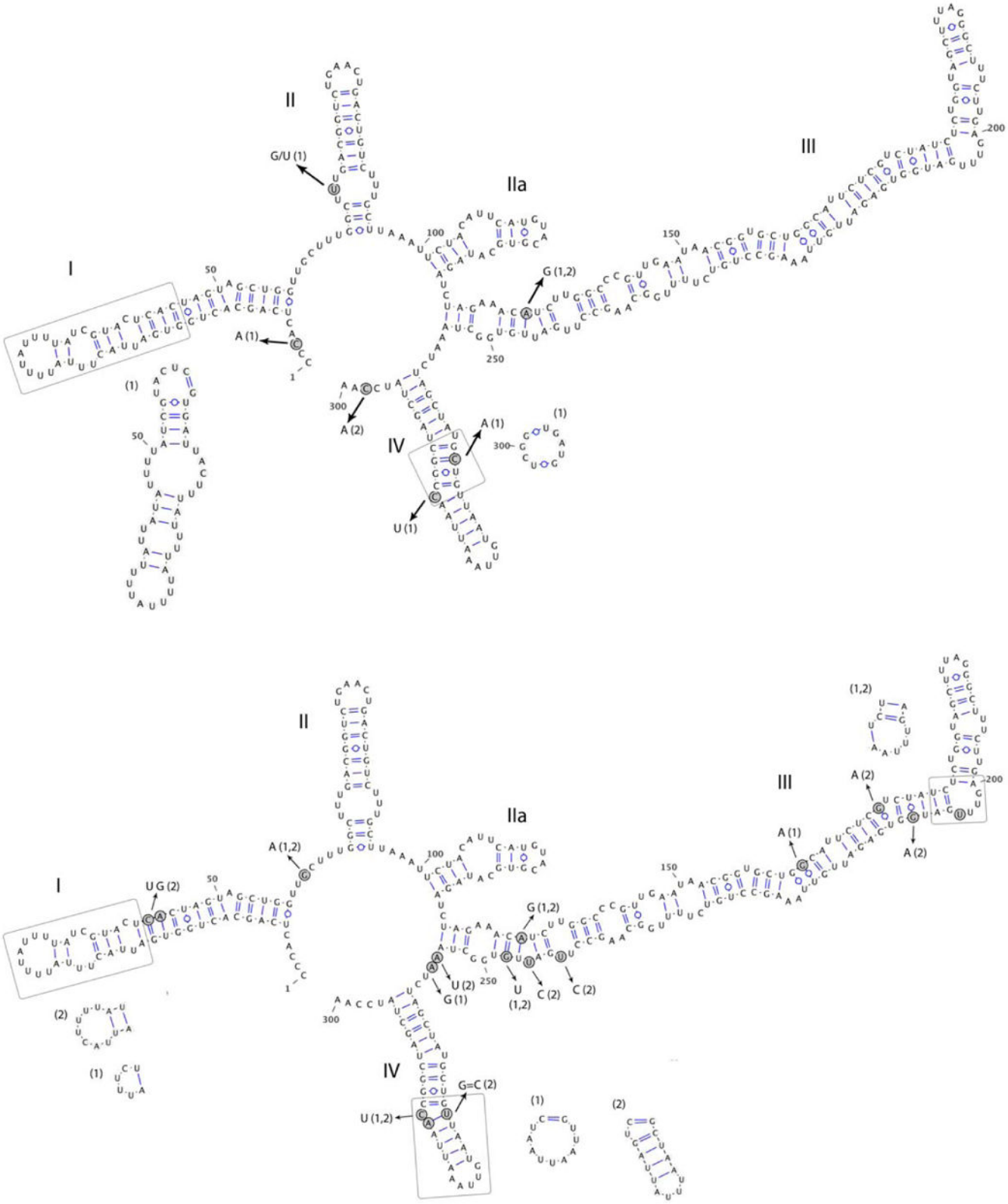

Figure 5.

(A – B). Diagrams of secondary structure of ITS2 rDNA of *P*. sp. GOM, compared with secondary structures of closely related taxa: (A) strains Hobart5 (1) and Ner-D6 (2); (B) strains Al-15 (1) and AL-17 (2). Base changes between *P*. sp. GOM and closely related taxa are shaded in gray, and boxes indicate changes in the structure and/or composition of particular sections of each helix.

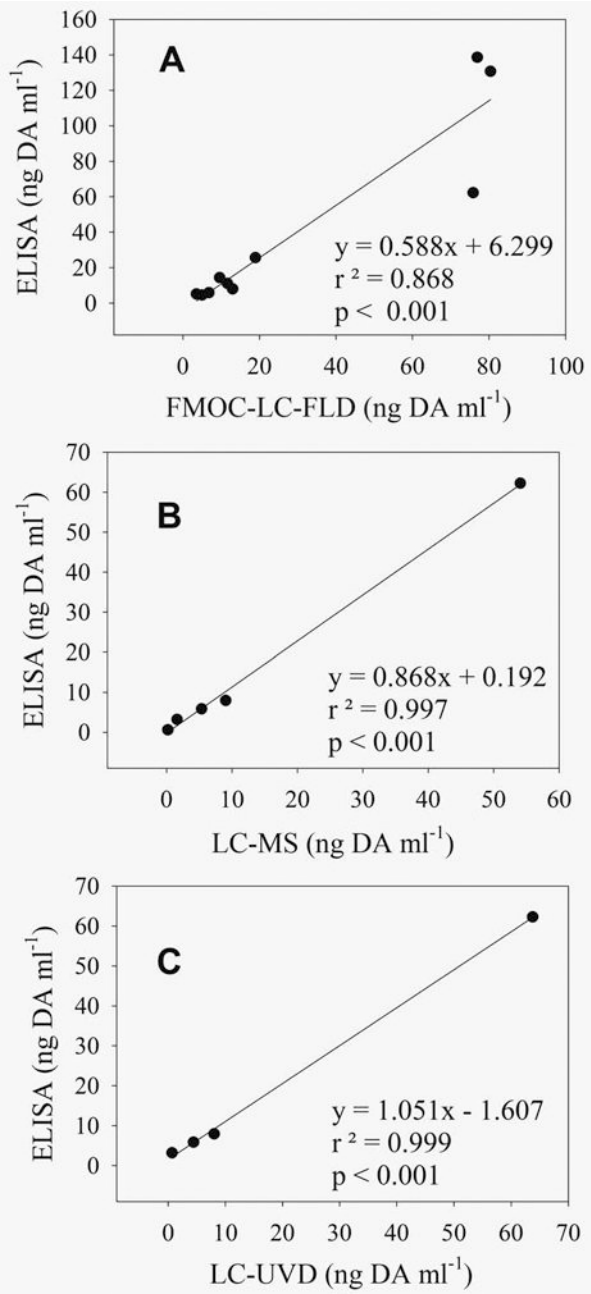

Figure 6.

(A - C). Concentrations of domoic acid in isolates of *Pseudo-nitzschia* spp. from the GOM. Extracts were analyzed by Biosense ASP ELISA and compared to more traditional analytical methods, including (A) FMOC-LC-FLD; (B) LC-MS; and (C) LC-UVD. Data are from Table 4.

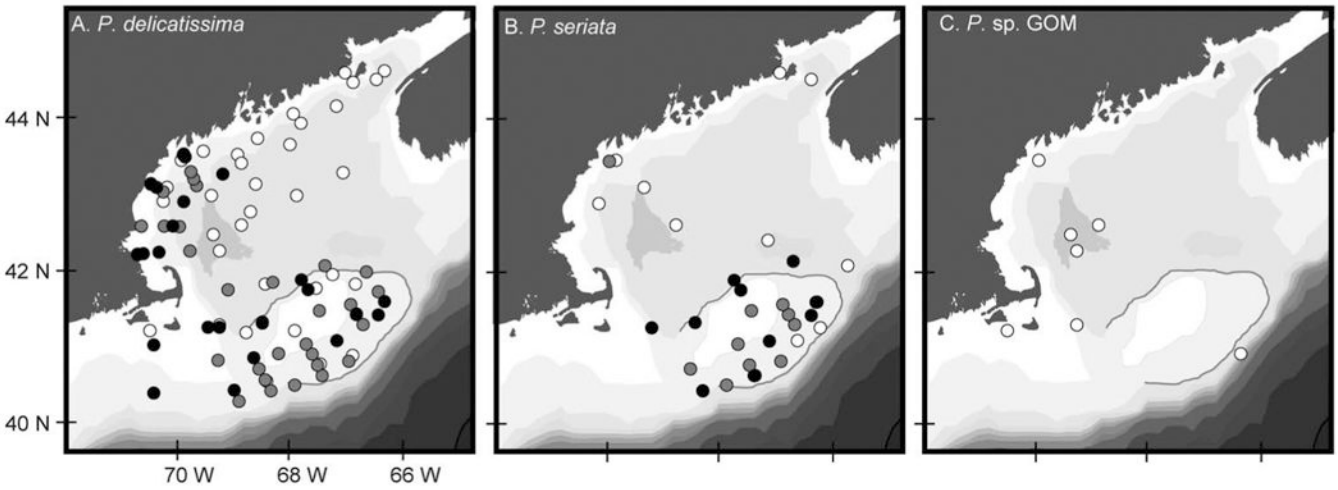

Figure 7.

(A-E). Observations of (A) *Pseudo-nitzschia delicatissima*; (B) *P. seriata*; and (C) *Pseudo-nitzschia* sp. GOM in the GOM, inferred either from successful isolations of these species or from electron microscopy-characterized field material.

Table 1

Summary of collection, identification and DA analyses conducted for *Pseudo-nitzschia* species isolated from the Gulf of Maine. A range of toxin concentrations is reported for each species; ranges encompass all isolates tested for each species, cultures in exponential, early and late stationary phase, and all detection methods. Cells were not separated from the growth medium prior to toxin analysis, and thus values represent intracellular + extracellular toxins.

Species	OC cruises observed[1]	Number of isolates	Number of stations where observed[2]	Identification method	Size group[3]	LSU GenBank accession	5.8S/ITS GenBank accession	DA analysis method	DA level (ng ml^{-1})
P. americana	440	NA	2	SEM	*americana*	NA	NA	NA	NA
P. delicatissima	440, 445, 447	66	23	SEM, sequence	*pseudo-delicatissima/delicatissima*	KF006832	KF006826	ELISA	0.11 - 0.39
P. fraudulenta	440, 445, 447	9	ND	SEM, sequence	*seriata*	KF006833	KF006827	ELISA	0.18 - 0.39
P. heimii	440, 447	3	ND	SEM	*seriata*	NA	NA	NA	NA
P. pungens	440	5	ND	SEM, sequence	*pungens*	KF006836	KF006830	ELISA, LC-MS, LC-UVD, FMOC-LC-FLD	0.04 - 1.1
P. seriata	440, 445, 447	26	7	SEM, sequence	*seriata*	KF006837	KF006824	ELISA, LC-MS, LC-UVD, FMOC-LC-FLD	1.4 - 140
P. subpacifica	440	8	1	SEM, sequence	*seriata*	KF006838	KF006831	ELISA, LC-MS, LC-UVD, FMOC-LC-FLD	0.06 - 1.1
P. turgidula	440, 445, 447	7	ND	SEM, sequence	*pungens*	KF006839	KF006825	ELISA	0.08 - 0.71
P. sp. GOM	440	11	1	SEM, TEM, sequence	*pseudo-delicatissima/delicatissima*	KF006835	KF006829	ELISA, LC-MS, LC-UVD, FMOC-LC-FLD	0.24 - 320

[1] Observations based on SEM identification only. Cruises occurred as follows: OC440 in October 2007, OC445 in April/May 2008 and OC447 in May/June 2008. The OC is left off cruise names in the table for brevity.

[2] Field observations are based on qualitative SEM detection in field material collected from 28 different stations (11 from OC440, 10 from OC445 and 6 from OC447).

[3] Based on light microscopy observations (see text).

NA: Not available.

ND: Not detected.

Table 2

Summary of morphological features of the *Pseudo-nitzschia* species recorded in the Gulf of Maine during the study period.

Species	Apical axis (µm)	Transapical axis (µm)	Striae in 10 µm	Poroids in 1 µm	Rows of poroids	Fibulae in 10 µm	Interspace	Valvocopula striae in 10 µm	Valvocopula poroids
P. americana	24-26	2.6	28-30	8-9	2	19-20	N	44-46	2 wide, 2-3 high
P. delicatissima	31-48	1.4-2.6	38-41	8-12	2	20-28	Y	46-52	1 (split in 3-4 sectors)
P. fraudulenta	64-84	5.2-6.2	22-23	5-6	2(3)	20-23	Y	38-40	2-3 wide, 8-12 high
P. heimii	81-92	5.2-5.4	29	8	2	17	Y	NA	2 wide, 3-4 high
P. pungens	72-149	3.0-4.1	10-12	3(4)	2	11-13	N	15-23	See appendix
P. seriata	53-134	5.3-6.3	17-20	7-8	3-4	15-18	N	23-24	2-3 wide, 4-5 high
P. subpacifica	36-68	3.8-5.8	29-33	8-9	2	17-21	Y	33-36	2 wide, 4-6 high
P. turgidula	31-69	3.0-4.0	2-23	7-9	1-2	13-18	Y	29-34	2 wide, 2-3 high
P. sp. GOM	30-54	1.5-2.1	39-42	5-6	1	21-26	Y	52-56	2 wide, 2-3 high

NA: Not available.

Table 3

Comparative morphometrics of *Pseudo-nitzschia* sp. GOM and species in the *P. pseudodelicatissima* complex.

Species	Apical axis (µm)	Transapical axis (µm)	Striae in 10 µm	Poroids in 1 µm	Poroid sectors	Fibulae in 10 µm	Valvocopula striae in 10 µm	Valvocopula poroids
P. sp. GOM	30-54	1.5-2.1	39-42	5-6	3-7	21-26	52-56	2 wide, 2-3 high
P. sp. Ner-D6[1]	NA	1.4-1.8	41-45	5-6	2-8	21-28	50-54	NA
P. sp. Hobart5[2]	60	1.4-1.6	38-40	3-5	>3	20-22	48-50	1 (split in 3-4 sectors)
P. pseudodelicatissima BOF[3]	54-80	1.2-2.1	38-43	5-6	3-4 (Type 1) 4-6 (Type 2)	20-27	54.5 (SD=2.7)	Similar to valve
P. caciantha[2]	53-75	2.7-3.5	28-31	3.5-5	4-5	15-19	33-38	2 wide 3-5 high
P. calliantha[2,4,5]	41-98	1.3-1.9	34-42	4-6	7-10	15-26	42-49	2-3 wide 4-5(6) high
P. cf. *calliantha*[6]	72-74	1.0-1.5	38-41	5-6	4-8	20-22	NA	NA
P. circumpora[7]	70.9-88.2	2.2-2.7	32-35	1-4	>7	15-19	40-42	NA
P. cuspidata[2]	30-72	1.4-2.0	35-44	4-6	2	19-25	47-53	1 (split in 2 sectors)
P. hasleana[8]	37-39	1.5-2.8	31-40	5-6	2-6	13-20	37-46	2 wide, 3-6 high
P. mannii[5,9]	33-130	1.6-2.6	30-40	4-6	2-7	17-26	46-48	2 wide 4(3) high
P. pseudo-delicatissima[2,5,9]	54-87	0.9-2.1	34-44	5-6	1-2	19-25	48-55	1 (split in 2 sectors)

[1] Orive et al., 2010;

[2] Lundholm et al., 2003;

[3] Kaczmarska et al., 2005;

[4] Quijano-Scheggia et al. 2008;

[5] Moschandreou et al., 2010a;

[6] Leandro et al., 2010;

[7] Lim et al. 2012;

[8] Lundholm et al., 2012;

[9] Amato and Montresor, 2008.

NA: Not available.

Table 4

Comparison of fg DA cell^{-1} domoic acid (DA) produced in culture for thirteen isolates of *Pseudo-nitzschia*, as determined by four detection methods: Biosense ASP ELISA, FMOC-LC-FLD, LC-MS and LC-UVD. Cells were not separated from medium prior to toxin analysis, and thus values represent total extracellular plus intracellular DA, standardized by the number of cells present at the time of culture harvesting.

Species	Isolate ID	ELISA (fg cell^{-1})	FMOC (fg cell^{-1})	LC-MS (fg cell^{-1})	LC-UVD (fg cell^{-1})
P. sp. GOM	Pn202-07 A8	21	34	24	21
P. sp. GOM	Pn202-07 F1	26	ND	8.6	ND
P. sp. GOM	Pn236-07 A3	110	ND	57	24
P. sp. GOM	Pn236-07 A4	150	180	130	150
P. sp. GOM	Pn236-07 F5	380	250	NA	NA
P. sp. GOM	Pn236-07 A2	19	21	NA	NA
P. sp. GOM	Pn237-07 C5	25	30	23	19
P. pungens	Pn295-07 B4	0.4	ND	ND	ND
P. seriata	Pn107-08 D1	130	89	NA	NA
P. seriata	Pn114-08 C2	3,500	1900	NA	NA
P. seriata	Pn114-08 D2	200	210	NA	NA
P. seriata	Pn120-08 A5	550	400	NA	NA
P. seriata	Pn149-08 D4	2,700	1600	NA	NA

NA: Not available; indicates sample was not analyzed by the indicated detection method.

ND: Not detected; indicates sample was analyzed by indicated method, but levels were below lower detection limits.

Table 5

Summary of domoic acid (DA) measurements associated with shellfish and marine mammals in Eastern N. American waters. Maximum values or a range are reported. PEI: Prince Edward Island; NB: New Brunswick; NS: Nova Scotia; QC: Quebec; NL: Newfoundland

Location	Date	Organism affected	*Pseudo-nitzschia* species	Toxin level (μg DA g^{-1})	Reference
Eastern PEI	Nov 1987	*Mytilus edulis*	*P. multiseries*	280-770[1] 810-1,500[2]	Bates et al., 1989
Eastern PEI	Dec 1987	*Mytilus edulis*	*P. multiseries*	145-345[1] 253-428[2]	Haya et al., 1991
Eastern PEI	Dec 1987	*Placopecten magellanicus*	*P. multiseries*	380-460[1] 2,600-4,180[2]	Haya et al., 1991
BOF-NB	Jul-Oct 1988	*Mytilus edulis*	*P. pseudodelicatissima*	74[1], 160[2]	Gilgan et al., 1990; Martin et al., 1990; Haya et al., 1991
BOF-NB	Jul-Oct 1988	*Mya arenaria*	*P. pseudodelicatissima*	33[1]	Gilgan et al., 1990
BOF-NS	Aug 1988	*Mytilus edulis*	*P. pseudodelicatissima*	8[1]	Gilgan et al., 1990; Martin et al., 1990
PEI	Nov 1988	*Mytilus edulis*	NR	350[1]	Gilgan et al., 1990
Eastern PEI	Nov 1988	*Mytilus edulis*	*P. multiseries*	280[1]	Bates et al., 1998
Eastern PEI	Fall 1989	*Mytilus edulis*	*P. multiseries*	16[1]	Bates et al, 1998
Eastern PEI	Fall 1990	*Mytilus edulis*	*P. multiseries*	0.6[1]	Bates et al., 1998
Northern PEI	Fall 1991, 1992, 1994, 2000, 2001	*Mytilus edulis*	*P. multiseries*	33[1]	Bates, 2004
GOM-Georges Bank	Apr-May 1995	*Placopecten magellanicus*	NR	>1300[2], 150[3]	Unpublished (see Stewart et al., 1998; Trainer et al., 2012)
GOM-Browns Bank	Apr-May 1995	*Placopecten magellanicus*	NR	4300[2]	Unpublished (see Stewart et al., 1998; Trainer et al., 2012)
BOF	Aug 1995	*Mya arenaria*	*P. pseudodelicatissima*	60[1]	Martin et al., 2004
Magdalen Islands, QC	Aug 1998	*Placopecten magellanicus*	NR	1.4-1.9[3]	Couture et al., 2001
Magdalen Islands, QC	Jun-Sep 1999	*Placopecten magellanicus*	*P. seriata* (in June)	0.84-24.6[2] (lagoon), 0.72-585[2] (offshore)	Couture et al., 2001; Levasseur et al., 2001
Magdalen Islands, QC	Jul 2000	*Placopecten magellanicus*	*P. seriata* (in June)	4.8[2] (lagoon), 265[2] (offshore)	Couture et al., 2001; Levasseur et al., 2001
St. Lunaire Bay, NL	Sep 2001	*Placopecten magellanicus*	NR	83[2]	Unpublished (CFIA)
Eastern NB, Northern PEI, Cape Breton Island, NS	Apr-May 2002	*Mytilus edulis*	*P. seriata*	71-200[1]	Bates et al., 2002; Bates, 2004
GOM-Georges Bank	Jul 2003	*Megaptera novaeangliae*	NR	NR	Pearson, 2003; NOAA press release NR03.15

Location	Date	Organism affected	*Pseudo-nitzschia* species	Toxin level (µg DA g^{-1})	Reference
Baie au Saumon QC	Jul-Oct 2004	*Placopecten magellanicus*	NR	39.2[5]	Unpublished (CFIA)
GOM-Georges Bank	2004-2005	*Placopecten magellanicus*	NR	9.9 or lower[4]	Day et al., 2008
GOM-Great South Channel	Apr-Jun 2005	*Eubalaena glacialis*	NR	0.175[6] or lower	Leandro et al., 2010
Baie au Saumon QC	Jun-Nov 2005	*Placopecten magellanicus*	NR	126.3[5]	Unpublished (CFIA)
BOF	Aug-Sep 2005	*Eubalaena glacialis*	*P. pungens*	0.171[6] or lower	Leandro et al., 2010
Baie Jacques-Cartier QC	Jul-Aug 2008	*Placopecten magellanicus*	*P. seriata*	119[5]	Unpublished (CFIA)
BOF-NB coast	Aug-Sep 2008	*Mytilus edulis*	NR	>20	Unpublished (CFIA)
GOM- eastern ME	Jul 2012	*Mytilus edulis*, *Mya* sp.	*P.* sp. GOM	5.8	Unpublished* (ME DMR, NOAA, FDA)

[1]Whole tissue shellfish sample.

[2]Digestive gland sample.

[3]Scallop roe sample.

[4]Scallop viscera.

[5]Scallop whole sample.

[6]Fecal sample.

PEI: Prince Edward Island; NB: New Brunswick; NS: Nova Scotia; QC: Quebec; NL: Newfoundland; ME: Maine. NR: not reported.

CFIA: Canadian Food Inspection Agency

ME DMR: Maine Department of Marine Resources

*Personal communication with A. Sirois, ME DMR